Inorganic Chemistry

Article

pubs.acs.org/IC

Solid State Structure of $Bi(N_3)_3$, $Bi(N_3)_3$·Solvates and the Structural Dynamics in the $[Bi(N_3)_6]^{3-}$ Anion

Kati Rosenstengel,[†] Axel Schulz,*[,†,‡] and Alexander Villinger*[,†]

[†]Abteilung Anorganische Chemie, Institut für Chemie, Universität Rostock, Albert-Einstein-Strasse 3a, 18059 Rostock, Germany

[‡]Leibniz-Institut für Katalyse e.V., Universität Rostock, Albert-Einstein-Strasse 29a, 18059 Rostock, Germany

Supporting Information

ABSTRACT: The highly explosive bismuth triazide, $Bi(N_3)_3$, was obtained in pure form by the reaction of BiF_3 with Me_3SiN_3 in acetonitrile under solvothermal conditions at temperatures between 90 and 100 °C. X-ray, ^{14}N NMR, infrared, and Raman spectra are discussed along with the data for the acetonitrile, acetone, and dmso adducts. The influence of the solvent on the purity of the azide products is studied in detail for $Bi(N_3)_3$ and the $[Bi(N_3)_6]^{3-}$ ion. Moreover, temperature dependent structural dynamics in the $[Bi(N_3)_6]^{3-}$ ion, which is caused by small changes in the local environment around the $[Bi(N_3)_6]^{3-}$ ion in the solid state, was studied by temperature variable single crystal X-ray and Raman studies. The azido-chlorido ligand back exchange was studied in detail by NMR techniques in $[Bi(N_3)_6]^{3-}$ and $Bi(N_3)_3$ when chlorinated solvents such as CH_2Cl_2 were utilized leading to the formation of $CH_2(N_3)Cl$ and/or HN_3 along with partially chlorinated bismuth azides.

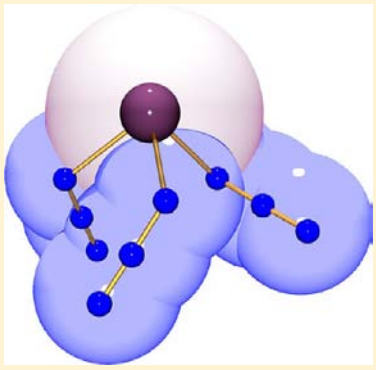

INTRODUCTION

The first report on binary bismuth(III)azide dates back to 1997 when Klapötke and A. Schulz published the IR spectrum of $Bi(N_3)_3$ taken from a mixture with AgI.[1] In 2010 the isolation of $Bi(N_3)_3$, $Bi(N_3)_3$·thf and salts containing $[Bi(N_3)_4]^-$ and $[Bi(N_3)_6]^{3-}$ ions was described by A. Schulz and Villinger.[2] However, only the latter two species could be structurally characterized as $[Ph_4P]^+$ salts. A year later S. Schulz et al. published the structure of $Bi(N_3)_3$·(pyridine)$_2$,[3] while Christe, Haiges, Rahm et al. (CHR) presented their results on $Bi(N_3)_3$, $[Bi(N_3)_4]^-$, and $[Bi(N_3)_6]^{3-}$ along with the novel $[Bi(N_3)_5]^{2-}$ and $[Bi(N_3)_5$·bipy$]^{2-}$ (bipy = 2,2′-bipyridine) ions as well as $[Bi(N_3)_3$·(bipy)$_2]_2$ in 2012.[4] Slightly earlier the synthesis and structure of $[Bi(N_3)_5$·dmso$]^{2-}$ was submitted by us.[5]

Organobismuth azides were known as early as 1934 when Challenger and Richards reported on the formation of $Ph_3Bi(N_3)_2$, which was obtained, when Ph_3BiCl_2 was treated with NaN_3.[6] At temperatures above 100 °C $Ph_3Bi(N_3)_2$ decomposes to give Ph_2BiN_3. Almost 40 years later Me_2BiN_3 was observed in the reaction of Me_3Bi with HN_3 and structurally characterized.[7] Dehnicke studied $BiON_3$ obtained from $Bi(NO_3)_3$ and NaN_3 in water by means of IR spectroscopy.[8] $Ph_3Bi(I)N_3$ was detected when IN_3 was treated with a solution of Ph_3Bi.[9] Recently, $[2\text{-}(Me_2NCH_2)C_6H_4]_2BiN_3$ and $[2\text{-}(Me_2NCH_2)C_6H_4]Bi(N_3)_2$ bearing the stabilizing 2-((dimethylamino)methyl)phenyl substituent were synthesized from iodide precursors by metathesis reaction with AgN_3.[10] The structures of both azide compounds were determined by single-crystal X-ray diffraction. While for the monoazide a monomeric species was found, the diazide dimerizes in the solid state exhibiting two bridging azido groups.

In general, bismuth azides are best synthesized by halogen/azide exchange reactions utilizing either the combination of bismuth iodide species and AgN_3 or bismuth fluoride species and Me_3SiN_3. For example, $Bi(N_3)_3$ can be prepared from BiI_3/AgN_3 or BiF_3/Me_3SiN_3 as depicted in Scheme 1.[2] The major problem in the synthesis of $Bi(N_3)_3$ is the preparation of pure and crystalline material since $Bi(N_3)_3$, obtained by these procedures at standard conditions, is either microcrystalline or almost amorphous, and it is rather difficult to isolate solvent-free $Bi(N_3)_3$. Therefore, characterization methods based solely on mass balances[4] (without elemental analysis) are to be avoided as they strongly depend on a complete conversion, a 100% selective reaction and solvent-free products. In such cases follow-up chemistry can hardly be carried out under correct stoichiometric conditions. The solvent problem arises from the

Scheme 1. Synthesis of $Bi(N_3)_3$[a]

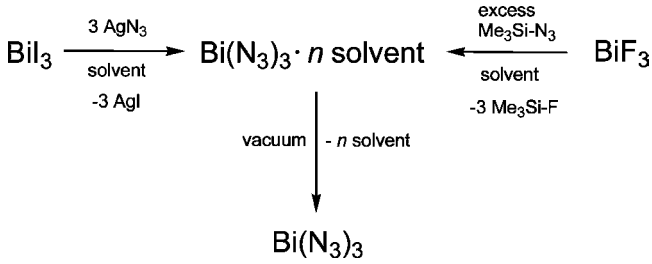

[a]1 atm, 298 K.

Received: February 26, 2013
Published: May 9, 2013

   dx.doi.org/10.1021/ic400493v | *Inorg. Chem.* 2013, 52, 6110−6126

Scheme 2. Synthesis of Salts Bearing Bismuth Azide Anions[a]

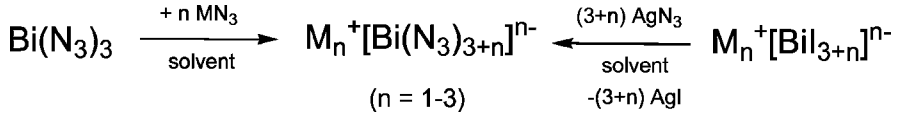

[a]M = weakly coordinating cation.

Table 1. Physical Data of Polyazidobismuth Compounds $M_n[Bi(N_3)_{3+n}]$, (M = weakly coordinating cation, n = 0−3)

compound	m.p./T_{dec} [deg]	^{14}N NMR [ppm] N_β $N_{\alpha/\gamma}$ $\Delta\nu_{1/2}$ (Hz) d_6-dmso	ν_{as} Raman [cm^{-1}]
$Bi(N_3)_3$	-/191[b]	*a*	2101, 2067, 2052
$Bi(N_3)_3$·dmso	-/200[b]	−137(71), −260(632)	2103, 2032, 2012, 2006
$Bi(N_3)_3$·acetonitrile	-/197[b]	*c*	2113, 2083, 2061, 2043
$Bi(N_3)_3$·acetone	-/227[b]	*d*	2118, 2085, 2044
$[Ph_4P][Bi(N_3)_4]$[h]	147/254	−136(43), −253(480)	2087, 2061, 2036, 2020
$[Ph_4P]_2[Bi(N_3)_5$·dmso$]$[h]	107/204	−135(47), −259(440)	2063, 2043, 2024
$[Ph_4P]_3[Bi(N_3)_6]$	179/285	−132(42), −258(390)	2063, 2025, 2007
$[EtPh_3P]_3[Bi(N_3)_6]$	143/218	−134(72), −260(547)	2093, 2058
$[Bu_4N]_3[Bi(N_3)_6]$	197/197	−133,[e] −262(230)	2056, 2003
$[Me_4N]_3[Bi(N_3)_6]$	*f*	−134(47), −265(320)[g]	*f*
$[Ph_4P]N_3$	235/-	−131(18), −276(52)	

[a]$Bi(N_3)_3$ completely dissolves in dmso from which the $Bi(N_3)_3$·dmso adduct can be isolated. [b]Detonation. [c]No resonances were observed in d_3-acetonitrile. [d]No resonances were observed in d_6-acetone. [e]Partially overlapping with CH_3CN at −135 ppm and resonance for $[Bu_4N]^+$ at −315 ($\Delta\nu_{1/2}$ = 2 Hz). [f]Only stable in solution. [g]Resonance for $[Me_4N]^+$ at −338 ($\Delta\nu_{1/2}$ = 2 Hz). [h]Taken from reference 5.

Scheme 3. Solvothermal Synthesis of $Bi(N_3)_3$

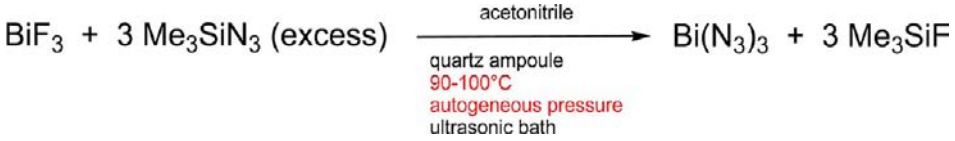

considerable Lewis acidity of BiX_3 halides and pseudohalides, respectively, leading to the formation of stable adducts such as $Bi(N_3)_3$·thf,[2] $Bi(N_3)_3$·(pyridine)$_2$,[3] or $[(bipyr)_2$·$Bi(N_3)_3]_2$ when donor solvents are used.[4] Here we will extend this adduct series by $Bi(N_3)_3$·acetonitrile, $Bi(N_3)_3$·acetone, and $Bi(N_3)_3$·dmso adducts. Even prolonged exposure to vacuum does often not lead to complete removal of the solvent. Less basic solvents such as CH_2Cl_2 can be fully removed; however, solubility problems are encountered (longer reaction times are needed) and CH_2Cl_2 as most other chlorinated solvents are not innocent with respect to a chlorido-azido ligand exchange which might lead to bismuth azide species with partial chlorine substitution, a problem we will address in detail in this paper.

Salts bearing binary bismuth−nitrogen anions of the type $[Bi(N_3)_4]^-$, $[Bi(N_3)_5]^{2-}$, and $[Bi(N_3)_6]^{3-}$ are easily obtained in reactions of $Bi(N_3)_3$ with stoichiometric amounts of MN_3 (M = weakly coordinating cation such as $[Ph_4P]^+$ and $[PNP]^+$; $[PNP]^+$ = Ph_3PNPPh_3) or stepwise when $[BiI_4]^-$/$[Bi(N_3)_4]^-$ or $[BiI_6]^{3-}$ is treated with stoichiometric amounts of AgN_3/MN_3 (Scheme 2). It is interesting to note that the attempted synthesis of a $[Ph_4P]^+$ salt containing the pentaazide anion $[Bi(N_3)_5]^{2-}$ led to the formation of a mixture of $[Bi(N_3)_4]^-$ and $[Bi(N_3)_6]^{3-}$ in a 1:1 ratio,[2] while the larger $[PNP]^+$ cation is capable of stabilizing the $[Bi(N_3)_5]^{2-}$ ion.[4] In contrast, the $[Ph_4P]^+$ salt containing the pentaazide dmso adduct anion $[Bi(N_3)_5$·dmso$]^{2-}$ can be obtained.[5] These salts containing bismuth−nitrogen anions are easy to handle as they are not shock-sensitive and dissolve readily in polar organic solvents (Table 1).

Here we present for the first time the isolation and structure of pure $Bi(N_3)_3$ utilizing solvothermal methods combined with an ultrasonic activation process. Moreover, we describe the temperature dependent structural dynamics in $[Bi(N_3)_6]^{3-}$, which is triggered by small changes in the local environment around the ion. This effect is studied by temperature variable single crystal X-ray and Raman studies. This work was mainly provoked by the severe criticism on our structural data and discussion of the $[Bi(N_3)_6]^{3-}$ ion expressed by CHR in their paper on bismuth(III) azides published 2012 in *Inorganic Chemistry*.[4] Here we want to give quite astonishing answers to their critical review, and we will prove that our previously published data regarding the $[Bi(N_3)_6]^{3-}$ ion are correct.[2]

RESULTS AND DISCUSSION

Synthesis and Structure of $Bi(N_3)_3$. As illustrated in Scheme 1, there are different ways to generate $Bi(N_3)_3$. So far it was impossible to obtain crystalline $Bi(N_3)_3$ by any of these methods applying standard reaction conditions ($T \leq 298$ K, 1 atm, solvents: thf, CH_3CN). Thus, we decided to change the thermodynamic parameters T and p in such a way that solvothermal reaction conditions were achieved (Scheme 3). For this reason, bismuth trifluoride BiF_3 suspended in acetonitrile and trimethylsilylazide, Me_3SiN_3, were combined at ambient temperatures in a quartz tube. The mixture was degassed several times, and the quartz tube was sealed in vacuo. Then this reaction mixture was heated at 90−100 °C in an ultrasonic bath for 10−12 h under autogenous pressure resulting in a yellow microcrystalline solid and a clear supernatant. The tube was opened in air and the suspension

dx.doi.org/10.1021/ic400493v | Inorg. Chem. 2013, 52, 6110−6126

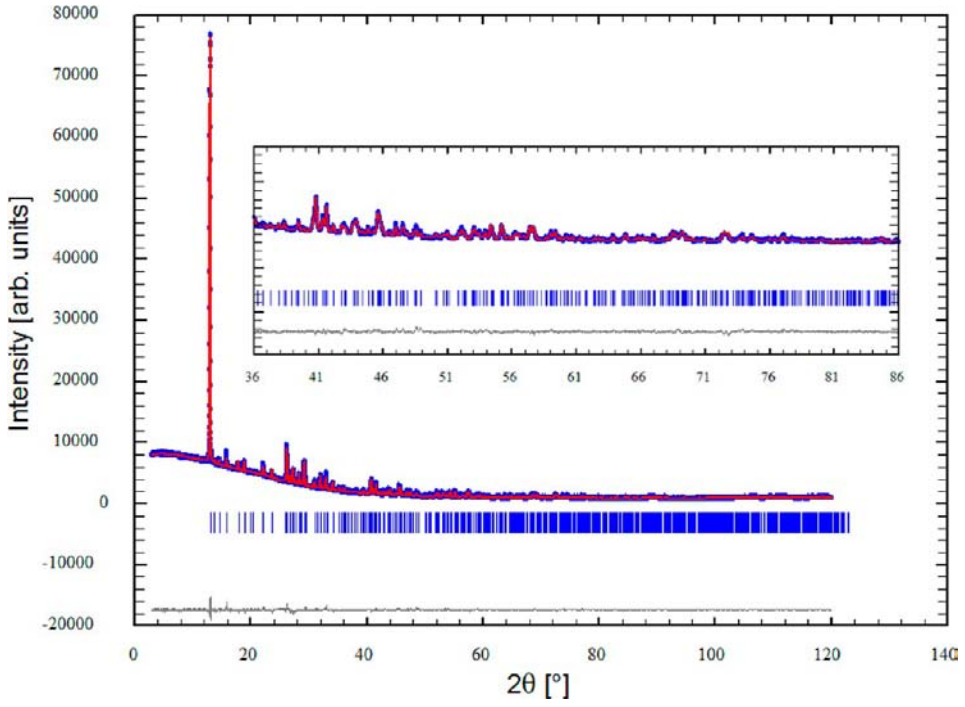

Figure 1. Observed and refined X-ray powder pattern of $Bi(N_3)_3$ (experimental pattern, blue line; calculated pattern, red line; vertical lines, Bragg positions; gray line, difference curve).

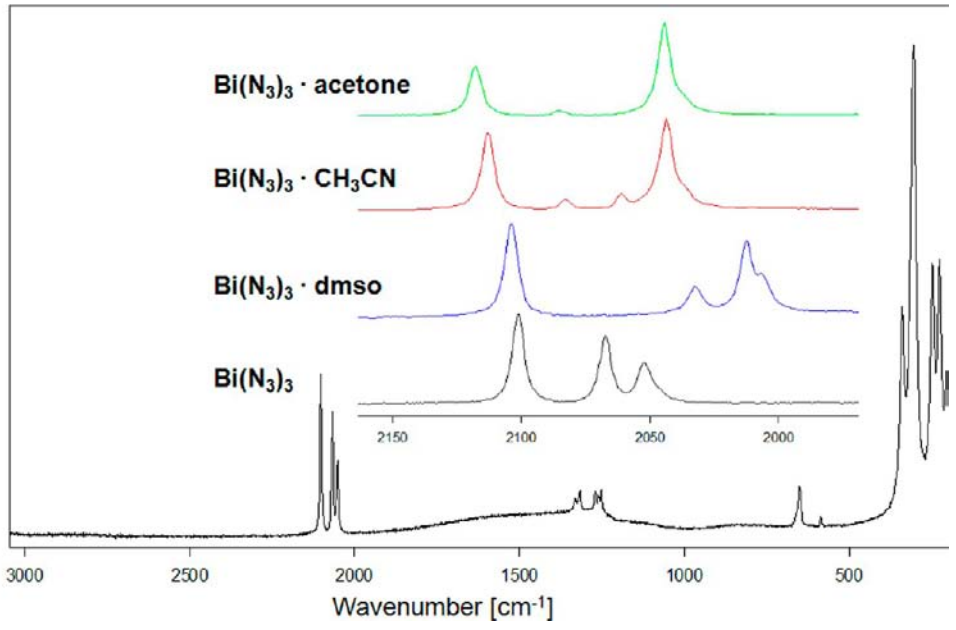

Figure 2. Bottom: Full Raman spectrum of pure $Bi(N_3)_3$. Top: Antisymmetric N_3 stretching modes (ν_{as,N_3}) in $Bi(N_3)_3$ (black), $Bi(N_3)_3$·dmso (blue), $Bi(N_3)_3$·acetonitrile (red) and $Bi(N_3)_3$·acetone (green).

transferred by syringe into a Schlenk tube. The supernatant is removed by syringe and the residue is washed with small portions of acetonitrile. Drying in vacuo gives bismuth triazide $Bi(N_3)_3$ as a yellowish crystalline solid in almost quantitative yields.

Caution! *Crystalline $Bi(N_3)_3$ synthesized solvothermally is extremely shock- and friction-sensitive and can explode violently upon the slightest provocation. Explosion occurred also once during the 12 h in the ultrasonic bath.*

Interestingly, small amounts of the $Bi(N_3)_3$·acetonitrile adduct could be isolated as colorless crystals from the supernatant acetonitrile upon cooling to ambient temperature. *Note*: Alternatively, the solvothermal synthesis can also be carried out without ultrasonic irradiation. However, X-ray quality single crystals were only obtained when ultrasonic irradiation was applied.

Solvothermally obtained, yellow crystals of $Bi(N_3)_3$ were suitable for single crystal X-ray diffraction (see below). The element composition of $Bi(N_3)_3$ was validated by ICP studies.

dx.doi.org/10.1021/ic400493v | *Inorg. Chem.* 2013, 52, 6110−6126

The phase purity was proven by powder diffraction experiments. As depicted in Figure 1, the experimentally observed and the theoretically calculated pattern are in very good agreement as demonstrated by Rietveld refinement and are in accord with the powder diffraction data of $Sb(N_3)_3$ which crystallizes isotypically.[3] Astonishingly, our powder diffraction data are totally different from those published by CHR.[4] Especially in the region $2\theta < 20°$ three intense reflections are observed for $E(N_3)_3$ (E = Bi, Sb); however, no reflections $2\theta < 20°$ are found in the diffraction pattern published by CHR.[4] Their published data did also not agree with the powder diffractogram of $Bi(N_3)_3$·acetonitrile (see Supporting Information, Figure S2). This prompted us to have a closer look at the powder diffraction data published by CHR.[4] Although only a figure (see Supporting Information of the CHR paper)[4] was available, it is obvious that the published CHR diffractogram corresponds mainly to the powder diffraction pattern of the starting material BiF_3 (in the space group *Pnma*, ICSD No. 1269) since most reflections are in good agreement with literature values (see Supporting Information, Figure S5).

Raman spectroscopy is particularly well suited to distinguish between pure $Bi(N_3)_3$ and $Bi(N_3)_3$·acetonitrile or any other solvent adduct (e.g., $Bi(N_3)_3$·dmso and $Bi(N_3)_3$·acetone, Figure 2). Even small amounts of solvent give rise to significant changes in the Raman spectrum of the pure compounds. For instance, three well-resolved antisymmetric N_3 stretching modes (ν_{as} N_3) at 2101, 2067, and 2052 cm^{-1} are observed in the Raman spectrum of pure $Bi(N_3)_3$ while four resolved bands are found for the acetonitrile (2113, 2083, 2061, 2043 cm^{-1}) and dmso adducts (2103, 2032, 2012, 2006 cm^{-1}) at different wave numbers. For $Bi(N_3)_3$·acetone only three bands are observed (2118, 2085, and 2044 cm^{-1}). So far only $Bi(N_3)_3$·solvent Raman data can be found in literature. Also the Raman data published by CHR agree nicely with our data for $Bi(N_3)_3$·acetonitrile but not with those of pure $Bi(N_3)_3$.[4]

^{14}N NMR spectroscopy is well suited to study azides in solution. To exclude chlorido-azido ligand back substitution chlorinated solvents should be avoided (see section Chlorido-Azido back-exchange). To dissolve significant amounts of $Bi(N_3)_3$ polar solvents such as dmso are needed. Because of dominant electrovalent bonding between the bismuth center and the azido group, only two resonances are found, a sharp signal at $\delta = -137$ ($\Delta\nu_{1/2} = 71$ Hz) for the N_β atoms and a broad resonance at $\delta = -260$ ($\Delta\nu_{1/2} = 632$ Hz) ppm for the $N_{\alpha,\gamma}$ atoms in accord with literature values (Table 1).[2] The observation of only one set of two azide signals and the absence of a separate N_α resonance also indicate strong quadrupole relaxation effects and a rapid ligand exchange on the NMR time scale.[11]

Single crystal X-ray studies were carried out for $Bi(N_3)_3$, $Bi(N_3)_3$·acetonitrile, $Bi(N_3)_3$·acetone, and $Bi(N_3)_3$·dmso. $Bi(N_3)_3$ crystallizes isostructurally to $Sb(N_3)_3$ (triclinic modification)[3,12] in the space group $P\bar{1}$ with two formula units per unit cell.[13] As depicted in Figure 3, the asymmetric unit consists of a C_1-symmetric $Bi(N_3)_3$ unit with the three azido groups arranged in a pyramidal, propeller-type fashion and three slightly different Bi–N_3 distances (Bi1–N4 2.301(6), Bi1–N7 2.313(7), and Bi1–N1 2.334(6) Å; cf. Σr_{cov}(Bi–N) = 2.22 Å).[14] It is interesting to note, that for $Sb(N_3)_3$ a second polymorph of $Sb(N_3)_3$ was published with ideal C_3-symmetric $Sb(N_3)_3$, which was found to crystallize in the rhombohedral space group $R\bar{3}$.[3,12] As for triclinic $Sb(N_3)_3$, no signs of a temperature dependent phase transition were detected for

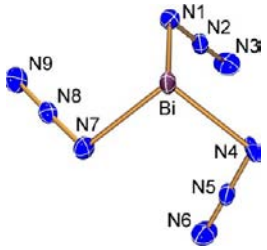

Figure 3. ORTEP drawing of the molecular structure of $Bi(N_3)_3$ in the crystal. Thermal ellipsoids with 50% probability at 173 K. Selected bond lengths (Å) and angles (deg): Bi1–N4 2.301(6), Bi1–N7 2.313(7), Bi1–N1 2.334(6), N1–N2 1.218(9), N2–N3 1.135(9), N4–N5 1.225(10), N5–N6 1.130(10), N7–N8 1.214(9), N8–N9 1.154(9); N4–Bi1–N7 87.2(2), N4–Bi1–N1 83.3(2), N7–Bi1–N1 83.1(2), N2–N1–Bi1 117.9(5), N5–N4–Bi1 114.9(5), N8–N7–Bi1 115.1(5), N3–N2–N1 178.5(8), N6–N5–N4 179.2(8), N9–N8–N7 178.4(9).

$Bi(N_3)_3$ which is always obtained as phase pure material (Figure 1).

The N–Bi–N angles are rather small (N4–Bi1–N7 87.2(2), N4–Bi1–N1 83.3(2), and N7–Bi1–N1 83.1(2)°) and the azide groups are almost linear which demonstrates strong electrovalent (besides contributions of covalent) bonding between the Bi and the N atoms. Highly polarized Bi–N bonds and dominant electrovalent bonding is corroborated by NBO/NRT analysis.[15,16] The N_α–N_β bond lengths in $Bi(N_3)_3$ (averaged 1.219 Å) are longer than the N_β–N_γ bond lengths (averaged 1.140 Å) as was observed for other $Bi^{(III)}$ azides (e.g., $[Bi(N_3)_4]^-$: 1.207 Å and 1.146 Å averaged values).[2]

A closer look at the intermolecular interactions (Figure 4, left) reveals an expansion of the Bi coordination number by the formation of nitrogen bridges involving the α-nitrogen atoms (N1, N4, and N7) of three adjacent azido ligands. This bridging mode results in the formation of four-membered Bi_2N_2 rings composed of two hexacoordinated bismuth and two bridging N_α atoms. Each bismuth atom is now surrounded by three of these four-membered rings. In addition, six of these four-membered rings are interconnected forming puckered 12-membered rings, with each four-membered ring being part of two of such 12-membered rings, thus forming infinite sheets of interconnected zigzag chains in the crystal (Figure 4 right, Figure 5 left). As illustrated in Figure 5, no significant interactions are observed between the puckered sheets. As shown below for the adducts, solvent molecules find space between these layers (Figure 5 right). One-dimensional zigzag chains were also observed in the crystal structure of $[Ph_4P][Bi(N_3)_4]$ which, however, are not interconnected.

The three Bi–N_{bridge} distances in $Bi(N_3)_3$ amount to Bi1–N7′ 2.578(7), Bi1–N4″ 2.649(6), and Bi1–N1‴ 2.685(6) Å (Figure 3, left), which is considerably shorter than the sum of the van der Waals radii of 3.62 Å.[17] Inspection of all Bi–N distances, which are smaller than the sum of the van der Waals radii (Table 2), revealed three additional close contacts (3.11–3.52 Å) indicating weak van der Waals interactions. Hence, the coordination around the Bi center in $Bi(N_3)_3$ can be best described as a [3 + 3] coordination leading to a two-dimensional network in the crystal. In addition these layers are interconnected by weak van der Waals contacts (two per Bi center, see above).

Synthesis and Structure of $Bi(N_3)_3$ Solvates. Synthesis of $Bi(N_3)_3$·dmso is easily achieved by the reaction of BiF_3 and

dx.doi.org/10.1021/ic400493v | Inorg. Chem. 2013, 52, 6110–6126

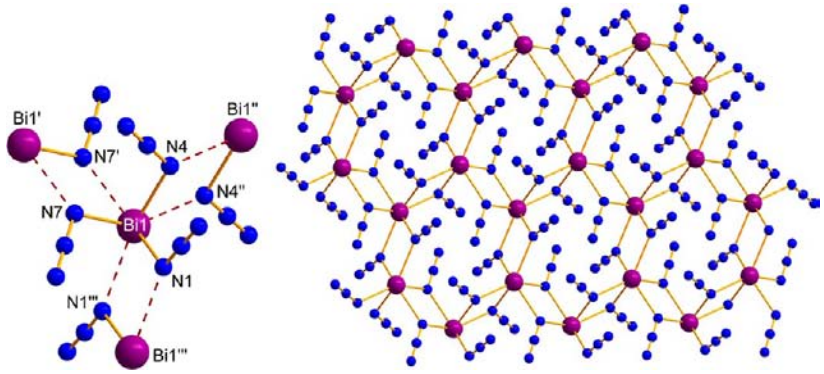

Figure 4. Ball-and-stick representation of the intermolecular interactions around one Bi atom in $Bi(N_3)_3$. Left: Structural motif. Right: Puckered sheet built from the structural motif. Selected bond lengths (Å): Bi1−N7′ 2.578(7), Bi1−N4″ 2.649(6), Bi1−N1‴ 2.685(6). Symmetry code: (′) $-x$, $-y$, $-z$; (″) $-x+1$, $-y$, $-z$; (‴) $-x$, $-y$, $-z+1$.

Me_3SiN_3 in dmso, which gives a clear yellow solution after 24 h. On the contrary, the synthesis of $Bi(N_3)_3$·acetonitrile and the $Bi(N_3)_3$·acetone adducts requires longer reaction times (4 days) leading to almost colorless solids. While crystals from the dmso solution can be obtained by concentration, crystals of $Bi(N_3)_3$·acetonitrile and $Bi(N_3)_3$·acetone were generated by heating a saturated solution under autogenous pressure.

Both the $Bi(N_3)_3$·acetonitrile and the $Bi(N_3)_3$·acetone adduct crystallize in the monoclinic space group $P2_1/c$ with four formula units per cell, while $Bi(N_3)_3$·dmso crystallizes in the triclinic space group $P\bar{1}$ with Z = 2. The phase purity of all adducts was proven by powder diffraction (Supporting Information, Figures S2−S4). The asymmetric units of all three compounds along with selected structural data are shown in Figures 6, 7, and 8. The structural parameters are in accord with those of $Bi(N_3)_3$ and other bismuth azides (see Supporting Information).[2−5] The donor−acceptor bond in the $Bi(N_3)_3$·acetonitrile adduct is rather long with 2.81(1) Å (cf. Σr_{cov}(Bi−N) = 2.22 Å, Σr_{vdW}(Bi···N) = 3.62 Å)[13,16] indicating a rather weak interaction, while a strong donor−acceptor bond is observed for $Bi(N_3)_3$·dmso with 2.391(2) Å (cf. Σr_{cov}(Bi−O) = 2.14 Å, Σr_{vdW}(Bi···O) = 3.59 Å).[13,16] For comparison, a considerably weaker Bi−O donor−acceptor bond is found in $[Bi(N_3)_5$·dmso$]^{2-}$ for which a Bi1−O1 donor−acceptor bond length of 2.879(4) Å is found.[5] The structure of $BiC1_3$·$(dmso)_2$ was published with shorter Bi−O distances of 2.345(9) and 2.39(1) Å.[18] A medium strong donor−acceptor bond is found in $Bi(N_3)_3$·acetone with 2.640(8) Å. Thus the strongest adduct with the shortest donor−acceptor bond is $Bi(N_3)_3$·dmso followed by $Bi(N_3)_3$·acetone.

In all three $Bi(N_3)_3$ adducts, an expansion of the Bi coordination number by the formation of nitrogen bridges involving the α-nitrogen atoms (N1, N4, and N7) of three adjacent azido ligands is also observed. Hence, in addition to the donor−acceptor bond, the main structural motif is the formation of three four-membered Bi_2N_2 rings surrounding each Bi center similar to the situation in solvent-free $Bi(N_3)_3$. However, the deviation from local C_3 symmetry is considerably more pronounced, but yet leading also to puckered 12-membered rings, which in turn form layers (Figures 5, 6−8). Between these layers either coordinating acetonitrile, acetone, or dmso molecules are found. In contrast to $Bi(N_3)_3$, all adducts display a coordination number of seven for the Bi centers, which leads to a much stronger puckering within the layers as displayed in Figure 5 right. A similar situation is found in $Bi(SCN)_3$·$1/2H_2O$ that consists of two-dimensional coordination networks with Bi centers which either bind to three sulfur, three nitrogen atoms, and to one oxygen atom or to four sulfur and three nitrogen atoms.[19]

Synthesis and Structure of $[Bi(N_3)_6]^{3-}$. Treatment of a stirred orange suspension of $[Ph_4P]_3[BiI_6]$ with an excess of silver azide, AgN_3, in acetonitrile at ambient temperatures yields after filtration and concentration a yellow viscous oil. Crystallization can be initiated by addition of a small crystal of $[Ph_4P]_3[Bi(N_3)_6]$ yielding $[Ph_4P]_3[Bi(N_3)_6]$ as a yellow crystalline solid in almost quantitative yield. Salts with other weakly coordinating monocations such as $[EtPh_3P]^+$, $[Me_4N]^+$ or $[Bu_4N]^+$ can be prepared accordingly (Scheme 4).[2] Interestingly, $[Me_4N]_3[Bi(N_3)_6]$ is stable in solution (as shown by ^{14}NMR spectroscopy, Table 1) but upon crystallization, only colorless crystals of $[Bu_4N]N_3$ can be isolated, while all other considered $[Bi(N_3)_6]^{3-}$ containing salts are easily obtained as yellow crystals. Crystals of $[Ph_4P]_3[Bi(N_3)_6]$ suitable for X-ray crystallographic analysis were obtained directly from the above reaction. Full characterization including single crystal X-ray studies, elemental analysis and ICP studies, ^{14}N NMR, IR and Raman studies were carried out to prove the elemental composition and structure of $M_3[Bi(N_3)_6]$. (Table 1 and see Supporting Information).

$[Ph_4P]_3[Bi(N_3)_6]$ crystallizes in the monoclinic space group $P2_1/n$ with four formula units per cell. No phase transition was observed in the considered temperature interval between 103 and 293 K. In the crystal there are no anion···anion contacts as they are completely separated by cations. As shown in Figure 9, each $[Bi(N_3)_6]^{3-}$ ion is C_1-symmetrically surrounded by 15 $[Ph_4P]^+$ ions.

The phosphorus atom of the cation sits in a slightly distorted tetrahedral environment with C−P−C bond angles between 105.8° and 111.7°. The averaged P−C bond lengths amount to 1.79 Å which corresponds to a typical single bond (cf. Σr_{cov}(P−C) = 1.86 Å).[13]

Figure 10 displays the molecular structure of the $[Bi(N_3)_6]^{3-}$ ion at 173 K with a strongly distorted octahedral BiN_6 skeleton. The most interesting structural feature is the disordered azido ligand with one significantly longer Bi−N16A (2.721(5) Å) and one significantly shorter Bi−N16B bond length (2.315(7) Å) as depicted in Figure 10 (middle).[20] The occupancy of each part was refined freely with 61.5% occupancy for the A and 38.5% for the B position. For $[Ph_4P]_3[Bi(N_3)_6]$, most of these data have been published recently by us.[2] The published X-ray data of $[Ph_4P]_3[Bi(N_3)_6]$ provoked CHR to severely criticize our structure discussion and put our data set into question.[4] They

dx.doi.org/10.1021/ic400493v | Inorg. Chem. 2013, 52, 6110−6126

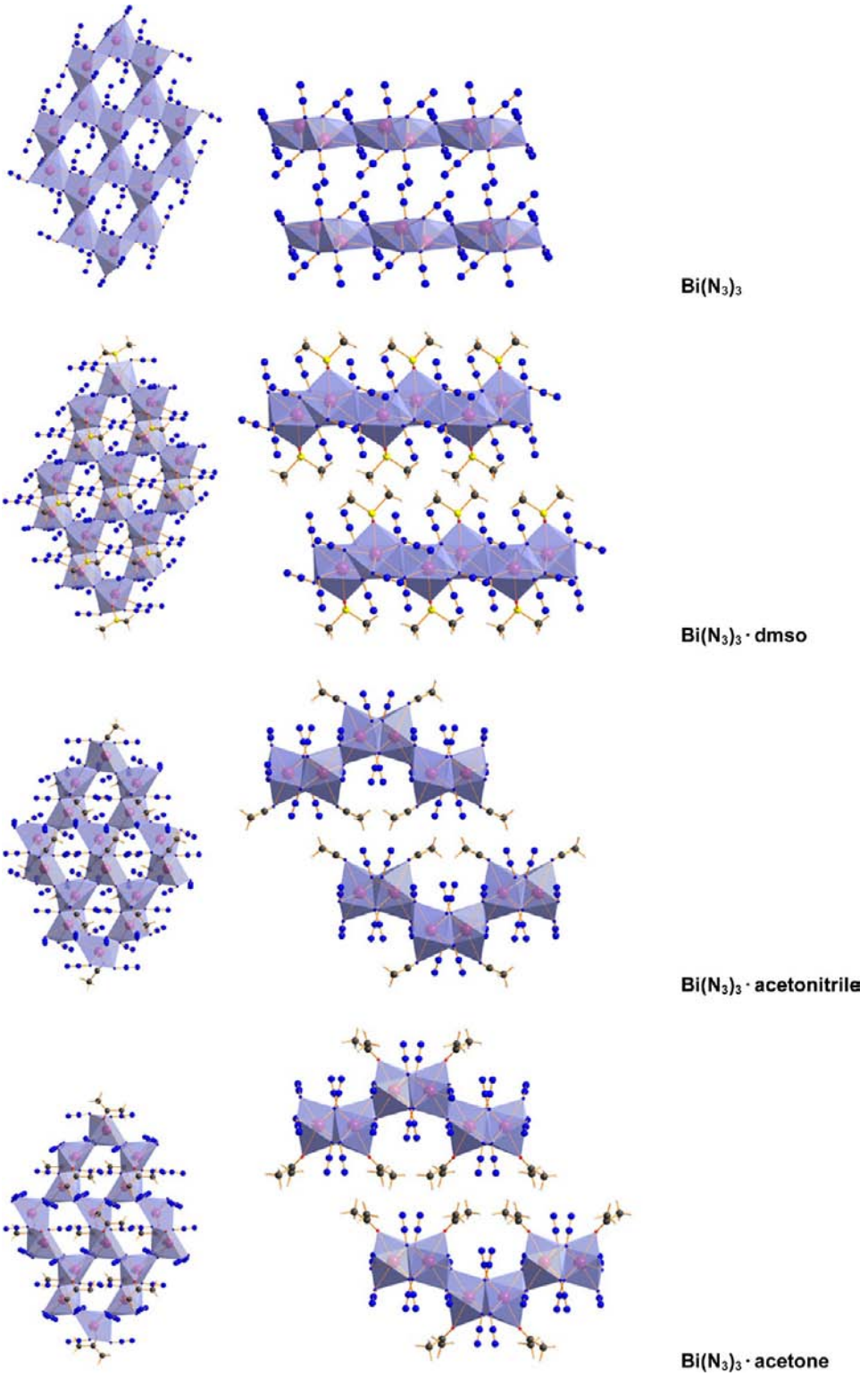

Figure 5. Left: Top view of the $Bi(N_3)_3$ layers. $Bi(N_3)_3$: view along *b*-axis, $Bi(N_3)_3$·dmso: view along *c*-axis, $Bi(N_3)_3$·acetonitrile: view along *a*-axis, and $Bi(N_3)_3$·acetone: view along *a*-axis. Right: Side view of two layers of two-dimensional networks composed of $Bi(N_3)_3$. $Bi(N_3)_3$: view along *a*/*c*-direction, $Bi(N_3)_3$·dmso: view along *b*-axis, $Bi(N_3)_3$·acetonitrile: view along *c*-axis, and $Bi(N_3)_3$·acetone: view along *c*-axis.

wrote ":... the reported structure of $[P(C_6H_5)_4]_3[Bi(N_3)_6]$ appears to be flawed. ... The Rostock group has reported very unusual bond distances of Bi–N16 = 2.719 Å[20a] and N17–N18 = 1.19 Å for the N16–N17–N18 azido ligand. These large deviations from the normal range of Bi–N distances are unexpected even for a disordered azido group but are similar to cases where an azido position is partially replaced by a chlorido ligand." Instead CHR published a Bi–N16 distance of 2.566(6) Å. When we read this criticism we were quite astonished as the whole synthetic procedure was carried out completely chlorine-free. The crystals were isolated from acetonitrile solution (vide supra).[21] Therefore, we thought that the difference between the

dx.doi.org/10.1021/ic400493v | *Inorg. Chem.* 2013, 52, 6110–6126

Table 2. Bi−N Distances [Å] of Polyazidobismuth Compounds $M_n[Bi(N_3)_{3+n}]$, (M = $[Ph_4P]$ or [PNP], n = 0−3)

	$Bi(N_3)_3$	$[Bi(N_3)_4]^{-a}$	$[Bi(N_3)_5]^{2-b}$	$[Bi(N_3)_6]^{3-a}$
network	2d	1d	no	no
Bi−N < 2.4	2.301(6)	2.273(2)	2.195(9)	2.32(2)
	2.313(7)	2.291(2)	2.361(6)	2.331(2)
	2.334(6)	2.377(2)	2.375(9)	2.364(2)
			2.381(8)	
Bi−N < 2.8	2.578(7)	2.449(2)	2.412(8)	2.478(2),
	2.649(6)	2.684(2)		2.487(2)
	2.685(6)	2.717(2)		2.719(5)
Bi−N < 3.6	3.114(7)	3.184(3)		
	3.276(9)	3.407(3)		
	3.515(9)			

[a]Values taken from reference 2. [b]Values taken from reference 4, $[PNP]^+$ cation

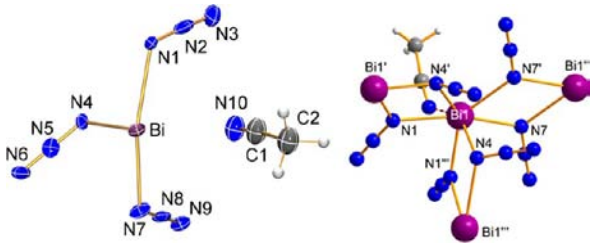

Figure 6. ORTEP drawing of the asymmetric unit $Bi(N_3)_3$·acetonitrile (left). Thermal ellipsoids with 50% probability at 173 K. Ball-and-stick representation of the main structural motif if intermolecular interactions are considered (right). Selected bond lengths (Å): Bi1−N4 2.28(1), Bi1−N1′ 2.40(1), Bi1−N7 2.46(1), Bi1−N1 2.50(1), Bi1−N7″ 2.582(1), Bi1−N4‴ 2.707(1), Bi1−N10 2.81(1), N1−N2 1.24(2), N2−N3 1.11(2), N4−N5 1.21(2), N5−N6 1.15(2), N7−N8 1.21(2), N8−N9 1.15(2). Symmetry codes: (′) x, $-y+3/2$, $z-1/2$; (″) $-x+1$, $-y+2$, $-z+2$; (‴) x, $-y+3/2$, $z+1/2$.

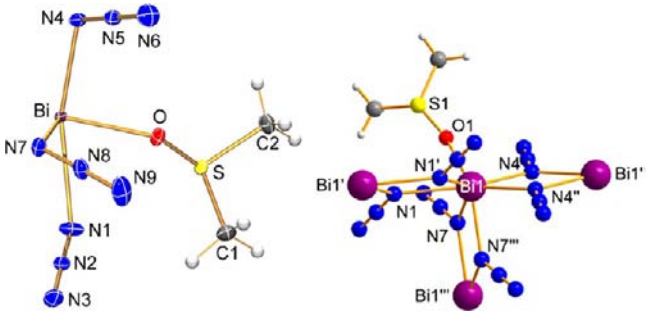

Figure 7. ORTEP drawing of the asymmetric unit in $Bi(N_3)_3$·dmso (left). Thermal ellipsoids with 50% probability at 173 K. Ball-and-stick representation of the main structural motif if intermolecular interactions are considered (right). Selected bond lengths (Å): N1−N2 1.201(3), Bi1−N1 2.591(2), Bi1′-N1 2.750(2), N2−N3 1.153(3), N4−N5 1.217(3), Bi1−N4 2.375(2), Bi1″-N4 2.631(2), N5−N6 1.141(3), N7−N8 1.226(3), Bi1−N7 2.454(2), N8−N9 1.132(3), S1−O1 1.532(2), Bi1−O1 2.391(2). Symmetry codes: (′) $-x+1$, $-y+1$, $-z+1$; (″) $-x+2$, $-y+2$, $-z+1$; (‴) $-x+1$, $-y+2$, $-z+1$.

data might be caused by a temperature effect since our published data were obtained at 173 K, while the CHR data set

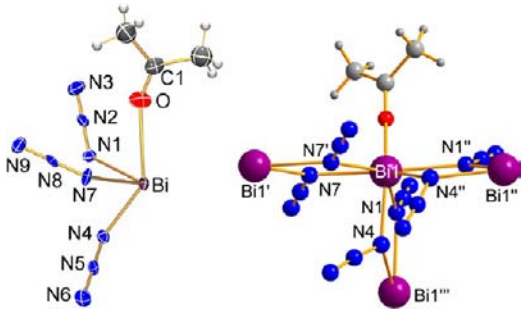

Figure 8. ORTEP drawing of the asymmetric unit in $Bi(N_3)_3$·acetone (left). Thermal ellipsoids with 50% probability at 173 K. Ball-and-stick representation of the main structural motif if intermolecular interactions are considered (right). Selected bond lengths (Å): Bi1−N4 2.316(8), Bi1−N1 2.422(8), Bi1−N7 2.468(7), Bi1−N1′ 2.497(8), Bi1−N7″ 2.565(8), Bi1−O1 2.640(8), Bi1−N4′ 2.657(8), N1−N2 1.22(1), Bi1‴-N1 2.497(8), N2−N3 1.13(1), N4−N5 1.22(1), N5−N6 1.11(1), N7−N8 1.209(9), N8−N9 1.17(1). Symmetry code: (′) x, $-y+1/2$, $z+1/2$; (″) $-x+1$, $-y$, $-z+2$; (‴) x, $-y+1/2$, $z-1/2$.

was measured at 143 K. In a next series of experiments we reproduced exactly our 173 K data set and then obtained a data set for 143 K. Also the data set at 143 K displayed similar structural parameters and exactly the same disorder (see Table 3) as detected at 173 K, which means, that we have not been able to reproduce the CHR data set published in the printed text of the paper. Therefore, we studied the cif-file published by CHR, which agrees surprisingly with our data set (Table 3), but absolutely disagrees with the data published in the printed text[4] with respect to the disorder. Moreover, it was impossible to draw the ORTEP representation of the $[Bi(N_3)_6]^{3-}$ ion published in the paper utilizing the published cif-file. To further illustrate this issue: CHR have used manipulated X-ray data[22] to criticize our previously published X-ray data of $[Ph_4P]_3[Bi(N_3)_6]$ although their published cif-file is in accord with our data with respect to the disorder. Besides, as shown in Table 3, our data set is of better quality as can be seen from the residuals (R_{int}/wR_2/GOF) although our data were obtained at significantly higher temperature (173 vs 143 K). Moreover, while our structure was refined without any restraints, CHR applied 55 restraints in the paper data, however, without giving any explanation why such a large number of restraints were introduced. In any case, our published data set is correct and describes the chlorine-free $[Bi(N_3)_6]^{3-}$ ion with the $[Ph_4P]^+$ cation as counterion. Nevertheless, this critique prompted us to carry out temperature variable X-ray measurements between 103−293 K in 10 K steps to gain further insight into the origin of this intriguing ligand disorder and to further validate our structural data.

The occupation of the A (B) position as a function of the temperature is depicted in Figure 11. From these data it can be derived that at low temperature the disorder disappears since 100% of isomer A is observed. With increasing temperature the occupation of the B position increases, that is, isomer B dominates the structure at T > 190 K. At T = 293 K more than 70% occupation of the B position is observed. Presumably, at larger temperature also 100% occupation of the B position will be reached. According to Boltzmann statistics the A isomer is energetically favored by about 6 kJ/mol (Figure 11 right and see Supporting Information).

dx.doi.org/10.1021/ic400493v | Inorg. Chem. 2013, 52, 6110−6126

Scheme 4. Synthesis of Salts Containing the $[Bi(N_3)_6]^{3-}$ Ion (M = Ph_4P, $EtPh_3P$, Bu_4N, and Me_4N)

$$M_3[BiI_6] + 6\,AgN_3\ (\text{excess}) \xrightarrow{CH_3CN} M_3[Bi(N_3)_6] + 6\,AgI$$

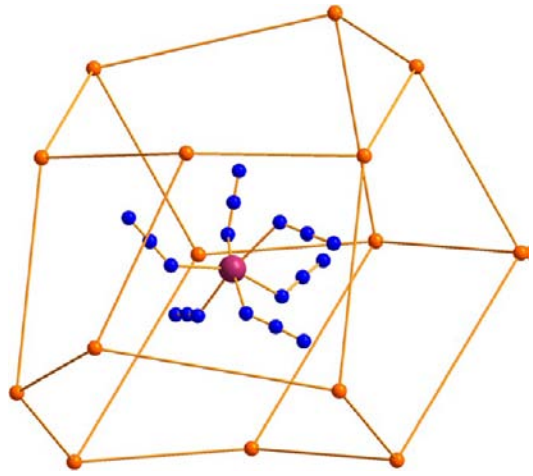

Figure 9. Cation arrangement around the $[Bi(N_3)_6]^{3-}$ ion in $[Ph_4P]_3[Bi(N_3)_6]$. Only the phosphorus atoms of the $[Ph_4P]^+$ ion are shown for clarity. Color code: P orange, N blue, Bi violet.

To understand the origin of the disorder problem it is worthwhile to have a closer look at the molecular structure of both isomers (Figure 12). For the high-temperature isomer B very similar (and rather short) Bi–N bond lengths in the range between 2.367(4) and 2.47(2) Å (cf. Σr_{cov}(Bi–N) = 2.22 Å, Σr_{vdW}(Bi···N) = 3.62 Å)[13,16] along with bond angles, which allow the formation of a "slightly" distorted BiN_6 skeleton (local O_h-symmetry), are observed. By contrast, for the low-temperature isomer A three shorter (Bi–N4 2.334(3), Bi–N7 2.347(3), and Bi–N13 2.316(3) Å) and three longer Bi–N distances (Bi–N1 2.527(3), Bi–N10 2.507(3), and Bi–N16 2.659(3) Å) are found. This situation resembles the situation in $Bi(N_3)_3$ and $[Bi(N_3)_4]^-$ since in both species an active lone pair localized at the $Bi^{(III)}$ center and a "strongly" distorted BiN_6 environment are found. Therefore, in our opinion, the long Bi–N16 distance of 2.659(3) Å is not unusual as it compares well with those for the Bi–N bridges in $[Bi(N_3)_4]^-$. This comment in our original paper from 2010, provoked CHR to write in their 2012 paper:[4] "The explanation given by the Rostock authors that the very long Bi–N16 distance might be due to a bridging azido ligand is unlikely because the anions in $[P(C_6H_5)_4]_3[Bi(N_3)_6]$ are very well separated from each other". Nowhere in our paper of 2010[2] have we discussed or graphically shown any anion···anion interactions or bridging azido ligands in the $[Bi(N_3)_6]^{3-}$ ion, all we wanted to do was to point out the similarities between these species with respect to the structural data. That is, the geometrical data of $[Bi(N_3)_4]^-$, $[Bi(N_3)_5]^{2-}$, and $[Bi(N_3)_6]^{3-}$ can also be referred to as complexes of $Bi(N_3)_3$ as displayed in the adduct formulations corresponding to, for example, $[Bi(N_3)_3{\cdot}3(N_3)^-]$, $\{[Bi(N_3)_4]^-{\cdot}2(N_3)^-\}$, or even $\{[Bi(N_3)_5]^{2-}{\cdot}(N_3)^-\}$ for isomer A of $[Bi(N_3)_6]^{3-}$.

With respect to the presence of two isomers exhibiting two different bond lengths, the same type of disorder was found in $[Bi(N_3)_5{\cdot}dmso]^{2-}$ with two significantly different Bi–O_{dmso} distances (isomer A with 62.4%: Bi–O 2.879(4) and isomer B with 37.6% occupancy: 2.582(6) Å).[5]

The presence of two different $[Bi(N_3)_6]^{3-}$ isomers in the solid state and the temperature depending occupation was also established by temperature variable Raman spectroscopy. Between 93 and 293 K Raman spectra were recorded in 10 K steps (see Supporting Information, Figure S28). The region between 1310 and 1330 cm^{-1} (region of the $\nu_{s,N3}$) is particularly well suited to distinguish between both isomers since no superposition with other vibrational modes is observed. With decreasing temperature an increasing intensity of the symmetric N_3 mode at smaller wave numbers, in which dominantly N16A–N17A–N18A are involved, is found. This results in considerable splitting of the symmetric N_3 mode at low temperatures.

Why is isomer A stabilized at low temperatures? From the structural data it can be deduced, that in the low-temperature isomer A the $Bi^{(III)}$ lone pair is sterically active pointing in the direction of the three distant azido ligands (Figures 13 and 14), while in isomer B the lone pair is sterically inactive. However, the lone pair does not directly point into the center of the triangle composed by the three distant azido groups in isomer A, but obviously more into the direction with the longest Bi–N distance (Bi–N16), which is corroborated by ELF computations as shown in Figures 13 and 14.[23] For comparison, the ELF was also plotted for isomer B and S_6-symmetric $[Bi(N_3)_6]^{3-}$ which represents the isomer with the highest possible symmetry and a sterically inactive lone pair at the Bi

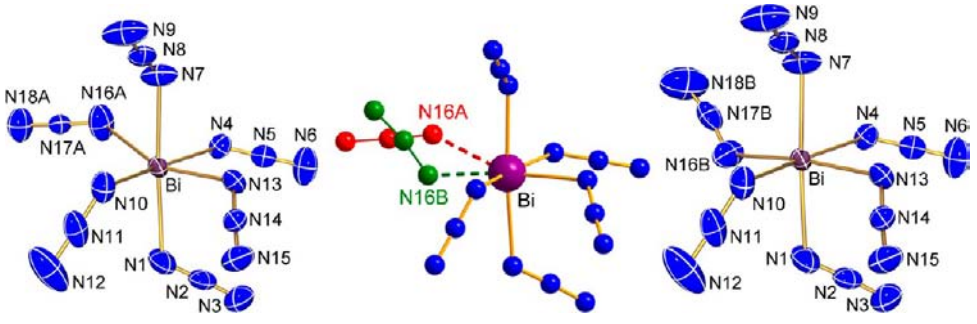

Figure 10. Left/right: ORTEP drawing of the molecular structure of the two isomers (A left/B right) of the $[Bi(N_3)_6]^{3-}$ ion in the crystal. Thermal ellipsoids with 50% probability at 173 K. Middle: Ball-and-stick drawing of the disorder. Selected Bi–N bond lengths (Å): Bi–N1 2.489(2), Bi–N4 2.41(1), Bi–N7 2.366(2), Bi–N10 2.480(2), Bi–N13 2.335(2), **Bi-N16A 2.721(5)** (red), **Bi-N16B 2.315(6)** (green).

dx.doi.org/10.1021/ic400493v | *Inorg. Chem.* 2013, 52, 6110–6126

Table 3. Comparison of Structural Data Obtained from Different X-ray Experiments

	Schulz/Villinger taken from ref 2	this paper	CHR paper taken from ref 4	CHR IC 2012 published cif file
T [K]	173	143	143	143
Bi−N1	2.487(2)	2.514(2)	2.482(4)	2.482(4)
Bi−N4[20]	2.32(2)	2.34(1)	2.339(4)	2.338(4)
Bi−N7	2.364(2)	2.356(2)	2.371(4)	2.370(4)
Bi−N10	2.478(2)	2.502(2)	2.476(4)	2.474(4)
Bi−N13	2.331(2)	2.325(2)	2.356(4)	2.355(3)
Bi−N16A	2.719(5)	2.688(3)	2.566(6)	2.728(10)
Bi−N16B	2.326(7)	2.33(1)	2.594(6)	2.426(9)
a [Å]	13.3271(3)	13.3124(3)	13.3429(9)	13.3429(9)
b [Å]	22.6255(6)	22.6514(5)	22.6779(16)	22.6779(16)
c [Å]	21.9806(6)	21.9590(5)	22.0466(15)	22.0466(15)
α [deg]	90	90	90	90
β [deg]	96.9230(10)	96.8410(10)	96.9480(10)	96.9480(10)
γ [deg]	90	90	90	90
V [Å^3]	6579.5(3)	6574.5(3)	6622.1(8)	6622.1(8)
measured reflections	92087	120682	56213	56213
independent reflections	19210	23833	14939	14939
reflections with $I > 2\sigma(I)$	13457	17566	14939[b]	9965
$R_{int.}$	0.0366	0.0400	0.0656	0.0656
$F(000)$	2984	2984	2984	2984
R_1 (R [$F^2 > 2\sigma(F^2)$])	0.0304	0.0327	0.0413	0.0400
wR_2 (F^2)	0.0574	0.0656	0.0802	0.0754
GoF	1.003	1.013	1.038	1.006
restraints	0	9[a]	55	14
parameters	903	903	866	866

[a]The geometry of the disordered azide groups was adjusted to reasonable NN distances (see _refine_special_details in the cif-file). [b]This value seems to be wrong.

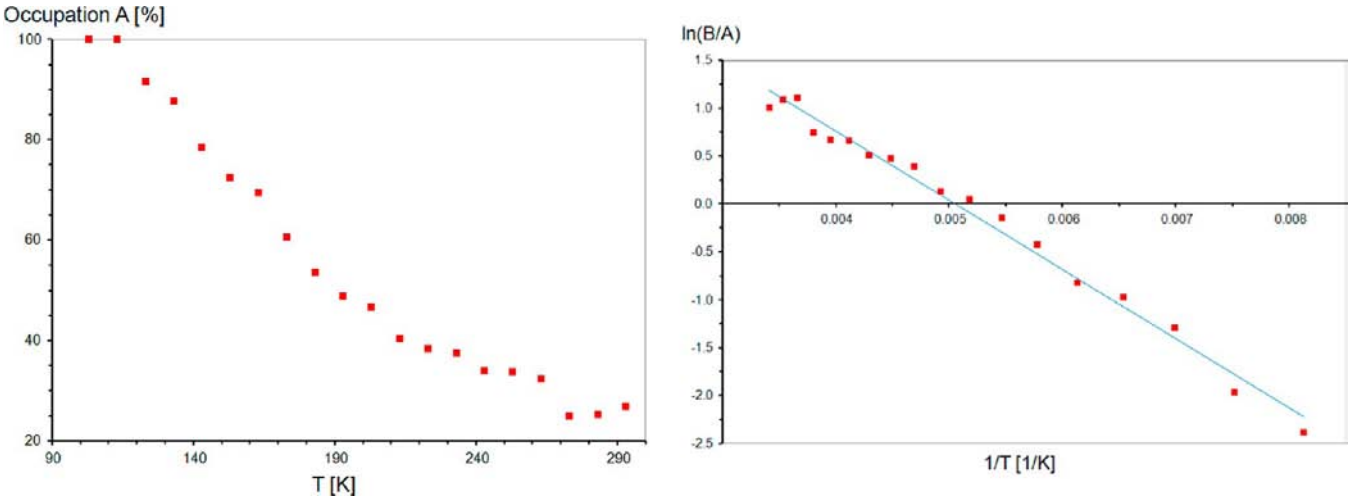

Figure 11. Left: Occupation probability of the A position as a function of the temperature (occupation of the B position = 100% − occupation of the A position); Right: Plot ln(B/A) vs $1/T$ [1/K].

center. The ELF for isomer B clearly displays an inactive lone pair which resembles the lone pair of the S_6-symmetric isomer.

In the 1950s Orgel explained lone pair effects by invoking mixing of s and p orbitals.[24] Natural bond orbital (NBO)[14,15] analysis of isomer A indicates that the sterically active lone pair possesses between 3 and 7% 6p orbital character (depending on the applied DFT method and structural data), while for isomer B and computed S_6-symmetric isomer the lone pair is located in 100% 6s orbital. Such small amounts of 6p character in the mathematical description of the lone pair may already result in stereochemical activity.

Owing to anharmonicity effects, with increasing temperatures the cell parameters increase as well as bond lengths and the size of cavities in accord with our temperature dependent data (see Figure 15, Supporting Information, Figures S9−S10). Two interesting exceptions were detected. While the longest Bi−N16A distance indeed increases, the other two longer Bi−N distances (Bi−N1, Bi−N10) decrease into the region of the

dx.doi.org/10.1021/ic400493v | Inorg. Chem. 2013, 52, 6110−6126

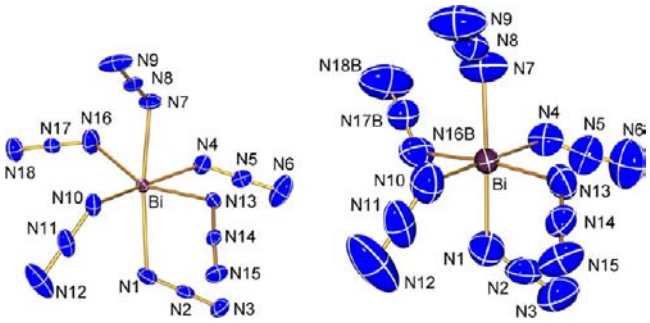

Figure 12. Left/right: ORTEP drawing of the molecular structure of the two isomers (A left/B right) of the $[Bi(N_3)_6]^{3-}$ ion in the crystal. Left: low-temperature isomer A at 103 K (100% occupancy). Right: high-temperature isomer B at 293 K (73% occupancy). Thermal ellipsoids with 50% probability. Bi–N bond lengths (Å): Isomer A: Bi–N1 2.527(3), Bi–N4 2.334(3), Bi–N7 2.347(3), Bi–N10 2.507(3), Bi–N13 2.316(3), Bi–N16 2.659(3); Isomer B: Bi–N1 2.414(3), Bi–N4 2.47(2), Bi–N7 2.419(3), Bi–N10 2.445(3), Bi–N13 2.387(3), Bi–N16B 2.367(4).

four shorter Bi–N distances (vide supra) with increasing temperature leading to six approximately similar Bi–N bond lengths. This corresponds to the fact that isomer B is stabilized at higher temperatures (Figure 11). Since at lower temperatures the volume of the C_1-symmetric cavity, which is composed of 15 $[Ph_4P]^+$ cations, significantly decreases by about 11% ($V^{(103K)}$ = 329.3 vs $V^{(293K)}$ = 371.6 Å^3, Figure 9), the interaction between the $[Bi(N_3)_6]^{3-}$ anion and the surrounding cations increases, obviously leading to a distortion of the approximate S_6 symmetry. Vice versa, at higher temperature the enlarged cavity allows a larger dynamics, resulting in six similar (shorter) bond lengths and higher symmetry for the anion, which adopts now a configuration, which resembles local S_6 symmetry. That is, the lone pair activity is triggered by small changes in the environment of the anion, which in turn are caused by a decrease of the temperature. Thus, it would be more adequate to speak of the azido ligand···cationic environment interaction as being stereoactive, while the lone pair plays only a passive role. Besides the cation···anion interactions, azido-ligand···azido-ligand repulsions and the energy gained by the expansion of the two nonbonding electrons into the valence shell play an essential role, so that the observed structure is a consequence of a very fine balance of all these interactions.[25]

The coordination shell of the lone-pair containing the Bi^{3+} ion can be treated as an invariant sphere with a uniform distribution of the ligands.[26] The inactive lone pair lies at the center of this sphere with overall S_6 symmetry. Under the temperature depending repulsion pressure some of the ligands are strongly bonding, they draw the cation toward them so that

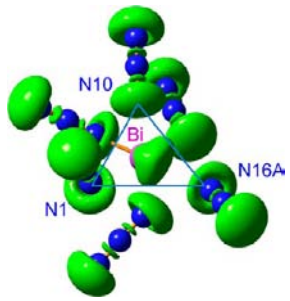

Figure 14. Three-dimensional representation (isosurface) of the ELF at 0.82 for isomer A, displaying the sterically active lone pair, which points toward the drawn triangle (N1, N10, and N16A).

the bonds to the stronger ligand become shorter (primary) while the bonds on the opposite side become longer (secondary) leading to a displacement of the Bi^{3+} from the center and decreasing symmetry. This simple model, introduced by Brown, allows dividing bonds into primary and secondary ones (see Table 2).[23]

In a fine theoretical paper Gérard et al. examined the thermal effects on the structure of the $[Pb(CO)_6]^{2+}$ complex utilizing dynamic calculations within the Car–Parrinello framework.[27] Astonishingly, they found very similar results for $[Pb(CO)_6]^{2+}$, which also exhibits a lone pair at the central Pb^{2+} center, compared to the $[Bi(N_3)_6]^{3-}$ ion: (i) Static computations revealed a high symmetry coordination (O_h symmetry), which is called a holodirected structure,[28] while dynamically, the picture is more complex with two groups of bonds, one group of three "short" bonds and one group of "long" bonds with one of the latest even exhibiting a very strong lengthening during the simulation. Large-amplitude and slow fluctuations of the distances are observed; most of the time one of the distances is much longer than the other five leading to a distorted AX_6E structure,[24] which is called hemidirected,[25] in accord with the experimental situation found in $[Bi(N_3)_6]^{3-}$. The ELFs of snapshots of the holo- (symmetric) and hemidirected (dissymmetric) structures are also in nice agreement with those of isomer A and B of $[Bi(N_3)_6]^{3-}$ as shown in Figures 13 and 14.[24]

According to the VSEPR model,[29] the $[Bi(N_3)_6]^{3-}$ ion belongs to the class of AX_6E molecules. Most known AX_6E molecules have an octahedral structure, but a few (e.g., $[SeF_6]^{2-}$, $[TeF_6]^{2-}$, $[IF_6]^-$, XeF_6) have a distorted octahedral structure (C_{3v} symmetry).[22] The C_{3v} distortion is described as a pseudo-Jahn–Teller effect.[30,31] As pointed out by Bersuker,[28] in particular, interatomic and molecular interactions generate bonded states of lower symmetry, that can be regarded as induced by a (pseudo-) Jahn–Teller type instability, which can

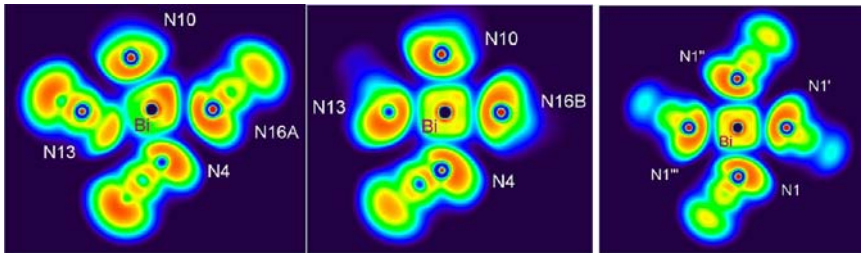

Figure 13. Two-dimensional cross section through the N16–Bi–N10 molecule plane of the electron localization function (ELF) Left: Isomer A, middle: Isomer B; right: S_6-symmetric isomer.

dx.doi.org/10.1021/ic400493v | Inorg. Chem. 2013, 52, 6110–6126

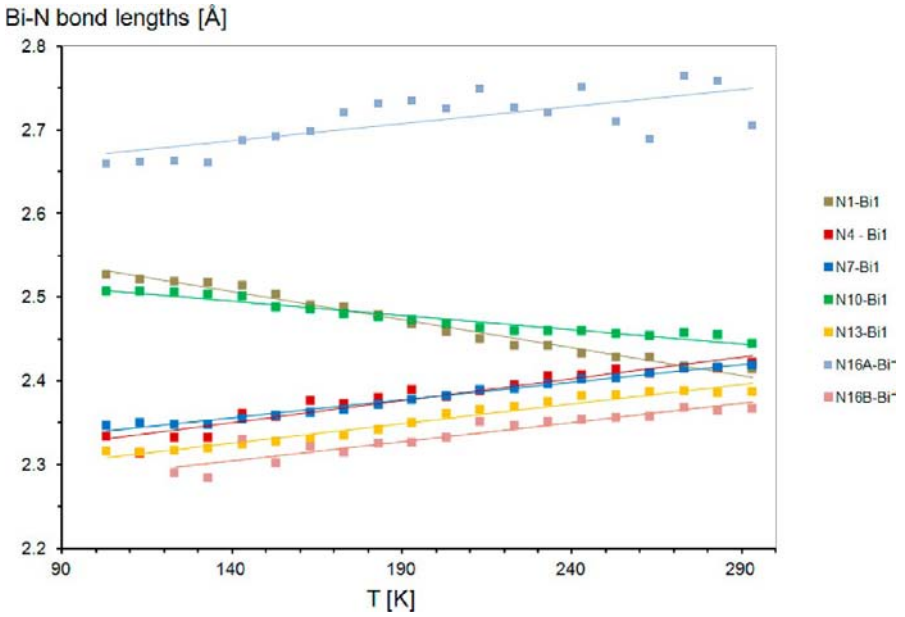

Figure 15. Bi–N bond lengths in $[Bi(N_3)_6]^{3-}$ as function of the temperature.

Scheme 5. Chlorido-Azido Ligand Back-Exchange Reactions When Chlorinated Solvents Are Used

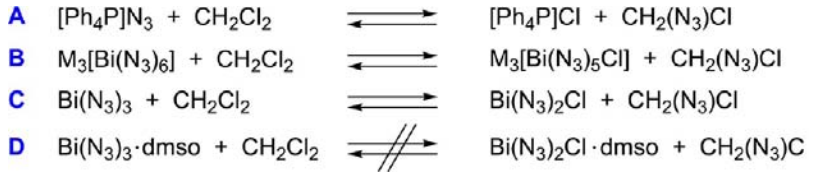

Table 4. ^{14}N NMR Data of Group 15 Azides, and for Comparison N_3^-, HN_3 and $CX_2(N_3)Cl$ and $CX(N_3)Cl_2$ (X = H, D)

species	chlorinated solvent	N_β in ppm ($\nu_{1/2}$ in Hz)	N_γ ($\nu_{1/2}$ in Hz)	N_α ($\nu_{1/2}$ in Hz)	reference
N_3^-	CD_2Cl_2	−129(17)	−277(44)	−277(44)	this paper
$CD_2(N_3)Cl$	CD_2Cl_2	−132(15)	−157(56)	−300(280)	this paper
$CH_2(N_3)Cl$	CH_2Cl_2/d_6-dmso	−134(30)	−162(100)	−300(600)	this paper
$CD(N_3)Cl_2$	$CDCl_3$	−138(22)	−148(80)	not observed	this paper
HN_3	CD_2Cl_2	−132(9)	−168(13)	−320(60)	this paper
HN_3	d_6-dmso	−134(20)	−255(400)	−255(400)	this paper
HN_3	Et_2O	−129	−174	−320	34
$As(N_3)_3$	CH_2Cl_2	−131	−165	−318	41,42
$Sb(N_3)_3$	CH_2Cl_2	−136(18)	−172(23)	−325(129)	12
$Sb(N_3)_3$	CH_2Cl_2	−134(26)	−169(34)	−321(170)	3
$Bi(N_3)_3$	CH_2Cl_2	−135(20)	−170(32)	−324(140)	3
$Bi(N_3)_3{\cdot}(pyridine)_2$	CH_2Cl_2	−135(25)	−172(480)	−325(580)	3

also be discussed for the $[Bi(N_6)]^{3-}$ structure dynamics. In this respect, molecular and intermolecular interactions may be regarded as a symmetry breaking which take place consequently by cooling the system.[28] All these AX_6E species have in common, that they have very flat potential energy surfaces, that is, small effects in the condensed phase may have a strong influence on the structure. As shown by Comba et al. for hexacoordinate copper(II) bispidine complexes two features emerge from the Jahn–Teller effect, (i) fluxionality and (ii) isomerism,[32] if asymmetric ligands (or asymmetry arising from the crystal lattice as in our case) lead to energetically and structurally distinct minima on the potential energy surface. A multiple (at least double) minima potential energy surface is the basis for distortional or bond-stretch isomerism. In this respect isomer A and B of the $[Bi(N_3)_6]^{3-}$ ion might be referred to as bond-stretch isomers.[33] In contrast to Comba's copper complex, a temperature-dependent equilibrium between the two isomers in $[Bi(N_3)_6]^{3-}$ is observed.

Chlorido-Azido Ligand Back-Exchange. Although it is known in literature,[34] that a chlorido-azido ligand back-exchange is possible, when chlorinated solvents such as CH_2Cl_2 are used in the azide preparation or crystallization process (Scheme 5), nothing is published about the kinetics. Only little is known on the conditions of such a side reaction in azide chemistry.[35,36] Since CHR mentioned this problem[4,31] in the context of the disorder problem with the $[Bi(N_3)_6]^{3-}$ ion

dx.doi.org/10.1021/ic400493v | Inorg. Chem. 2013, 52, 6110–6126

structure (and although it was clear that the origin of the disorder was definitely not associated with a chloride exchange), we tackled the problem in a series of experiments: (i) crystallization studies with $[Ph_4P]_3[Bi(N_3)_6]$ in CH_2Cl_2 and (ii) ^{14}N, ^{1}H, and ^{13}C NMR studies with $[Bi(N_3)_6]^{3-}$ salts and $Bi(N_3)_3$ along with blind experiments utilizing $[Ph_4P]N_3$ and HN_3. The latter experiments were carried out, since we have been puzzled for a long time by the fact that for many different main group azide species bearing heavy elements very similar (often identical) ^{14}N NMR data were reported (Table 4).

Cl^-/N_3^- Exchange in $[Bi(N_3)_6]^{3-}$. Alternatively to the crystallization in acetonitrile (vide supra), the crystallization can be carried out in CH_2Cl_2, which for example avoids the formation of a viscous oil. However, to exclude any azido/chlorido ligand exchange the use of acetonitrile is recommended. Crystals obtained from a concentrated CH_2Cl_2 solution after storage for several days at ambient temperature were found to be slightly contaminated by chloride ($[Ph_4P]_3[Bi(N_3)_{5.88}Cl_{0.12}]$), while short crystallization times did not lead to a measurable Cl^- contamination in the structural data. As shown in Figure 16, the molecular structure

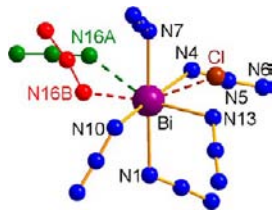

Figure 16. Ball-and-stick drawing of the N16A/N16B disorder problem along with the partial chlorine occupation in $[Ph_4P]_3[Bi(N_3)_{5.88}Cl_{0.12}]$ (cation omitted for clarity). Selected bond lengths (Å): Bi–N1 2.473(3), Bi–N4 2.41(2), Bi–N7 2.385(2), Bi–N10 2.446(3), Bi–N13 2.352(3), **Bi-N16A 2.757(5)** (red), **Bi-N16B 2.320(6)** (green), **Bi–Cl 2.87(2)** (brown).

of this chlorine contaminated anion revealed exactly the same disorder problem as discussed before for pure $[Bi(N_3)_6]^{3-}$, and the structural parameters are very similar, another proof that chlorine contamination can be ruled out to be responsible for the disorder in $[Ph_4P]_3[Bi(N_3)_6]$.

In a next series of experiments we studied the chlorido-azido ligand exchange by means of NMR techniques starting from chlorine-free compounds. At first $[Ph_4P]N_3$ was dissolved in neat CD_2Cl_2 (Scheme 5, reaction A). After 30 min the ^{14}N and ^{1}H NMR spectra documented already the expected N_3^-/Cl^- exchange, since three new resonances at $\delta = -132$ (N_β, $\Delta\nu_{1/2}$ = 15 Hz), −157 (N_γ, $\Delta\nu_{1/2}$ = 56 Hz), and −300 ppm (N_α, $\Delta\nu_{1/2}$ = 280 Hz) besides the two for the N_3^- ion at $\delta = -129$ (N_β, $\Delta\nu_{1/2}$ = 17 Hz) and −277 ($N_{\alpha/\gamma}$, $\Delta\nu_{1/2}$ = 44 Hz) were found in the ^{14}N NMR spectrum (Figure 17) and one new resonance at δ = 5.28 for $CDH(N_3)Cl$ in the ^{1}H spectrum besides those expected for the phenyl groups of the cation and $CDHCl_2$ indicating the formation of azidochloromethane (cf. $CH_2(N_3)Cl$ ^{1}H NMR: 5.0 ppm in $CDCl_3$).[33] Now the same reaction was carried out in d_6-dmso with stoichiometric amounts of CH_2Cl_2 and $[Ph_4P]N_3$ (Scheme 5, reaction A). Over a period of 36 days ^{1}H, ^{13}C, and ^{14}N NMR spectra were measured (see Supporting Information, Figures S12–S14). The experimental data for the exchange reaction in CH_2Cl_2 with N_3^- (reaction A in Scheme 5) indicate a reversible reaction for the forward and reverse directions with both reactions following a second order rate law. As depicted in Figure 18, for a second order rate law the mathematical model agrees nicely with the experimental data and rate constants of 8.07×10^{-3} (forward) and 9.40×10^{-3} $L \cdot mol^{-1} \cdot h^{-1}$ (reverse direction) could be derived. The same experimental setup was applied for (chlorine-free synthesized) $[EtPh_3P]_3[Bi(N_3)_6]$, which was first dissolved in d_6-dmso and then treated with stoichiometric amounts of CH_2Cl_2 (Scheme 5, reaction B). At the beginning of the reaction only the two resonances for $[Bi(N_3)_6]^{3-}$ ion (−134 (N_β, $\Delta\nu_{1/2}$ = 72 Hz) and −260 ppm ($N_{\alpha/\gamma}$, $\Delta\nu_{1/2}$ = 547 Hz)) were observed in the ^{14}N NMR spectrum but again after 16 h the resonances of $CH_2(N_3)Cl$ could be detected (Supporting Information, Figure S16). According to time-dependent ^{1}H NMR data it is evident that, at the beginning of the reaction, the exchange follows also a second-order rate law. However, the kinetic model becomes more complex since a consecutive reaction due to multiple

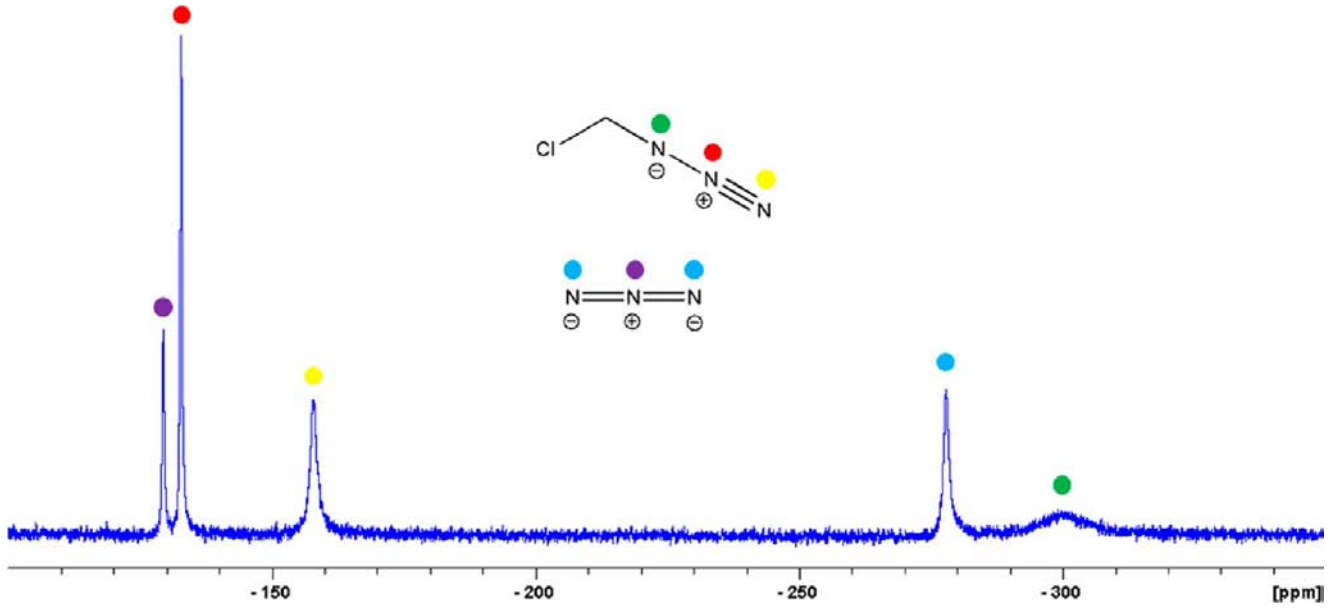

Figure 17. ^{14}N NMR spectrum of the reaction solution of $[Ph_4P]N_3$ with excess CD_2Cl_2.

dx.doi.org/10.1021/ic400493v | Inorg. Chem. 2013, 52, 6110–6126

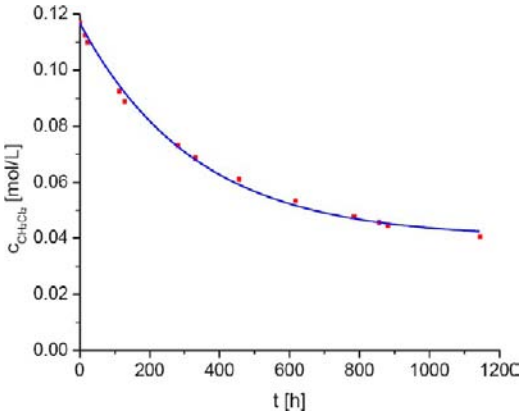

Figure 18. Kinetics of the Cl^-/N_3^- ligand back exchange for reaction A in Scheme 5 (red, experimental data; blue, modeled data according to second order rate law).

azido ligand dissociation of $[Bi(N_3)_6]^{3-}$ ion was observed (Supporting Information, Figure S17). When $[Ph_4P]_3[Bi(N_3)_6]$ was dissolved in neat CD_2Cl_2 the formation of $CDH(N_3)Cl$ (−134 (N_β, $\Delta\nu_{1/2}$ = overlapping with N_β of $[Bi(N_3)_6]^{3-}$), −158 (N_γ, $\Delta\nu_{1/2}$ = 50 Hz), and −300 ppm (N_α, $\Delta\nu_{1/2}$ = 290 Hz)) was observed at once (Figure 19, measured after 30 min) besides the two resonances expected for $[Bi(N_3)_6]^{3-}$ (−133 (N_β, $\Delta\nu_{1/2}$ = 28 Hz) and −258 ppm (N_γ, $\Delta\nu_{1/2}$ = 250 Hz)).

Cl^-/N_3^- Ligand Back Exchange in $Bi(N_3)_3$. Finally, we treated a solution of $Bi(N_3)_3$ in d_6-dmso with stoichiometric amounts of CH_2Cl_2 (Scheme 5, reaction D); however, in this case no azido/chlorido ligand back exchange was detected even after two weeks. For this reason we prepared a suspension of $Bi(N_3)_3$ in neat CH_2Cl_2, and NMR spectra were recorded over a period of 48 days (Scheme 5, reaction C; Supporting Information, Figure S19). After three days the formation of a new azide species could be clearly verified on the basis of its ^{14}N NMR data (δ = −133 (N_β, $\Delta\nu_{1/2}$ = 8 Hz), −169 (N_γ, $\Delta\nu_{1/2}$ = 13 Hz), and −321 ppm (N_α, $\Delta\nu_{1/2}$ = 100 Hz)) which, however, were significantly different from those of $CH_2(N_3)Cl$ (δ = −134 (N_β, $\Delta\nu_{1/2}$ = 30 Hz), −162 (N_γ, $\Delta\nu_{1/2}$ = 100 Hz), and −300 ppm (N_α, $\Delta\nu_{1/2}$ = 600 Hz)). Although the difference in the chemical shifts is rather small, especially the half widths are very indicative to distinguish between both species. Additionally, the ^1H NMR spectrum revealed a new, very broad resonance at 4.53 ppm. Therefore we assumed the slow formation of HN_3 which was unequivocally proven in ^{14}N and ^1H NMR experiments of freshly prepared HN_3 dissolved in CH_2Cl_2 (^{14}N NMR: −132 (N_β; $\Delta\nu_{1/2}$ = 9 Hz); −168 (N_γ; $\Delta\nu_{1/2}$ = 13 Hz); −320 (N_α; $\Delta\nu_{1/2}$ = 60 Hz); cf. HN_3 in diethyl ether: −129, −174, and −320 ppm).[37] In conclusion, problems with NMR data may arise either from azido ligand dissociation in dominantly ionically bonded azidometallates (e.g. $[Bi(N_3)_6]^{3-}$) or badly soluble azides in combination with chlorinated solvents along with long NMR measuring times (Table 4). Additionally, slow formation of HN_3 must be considered when acidic solvents such as CH_2Cl_2 are used. Presumably, in these cases the chlorido-azido exchange is triggered by the intermediate formation of, for example, HCl, and no azidomethane is observed. Both azide forming decomposition reactions (azidomethane and HN_3) must be considered when dealing with ^{14}N NMR data, especially of unknown species. Both reactions might even be superimposed. With the ^{14}N NMR data of azidomethane and HN_3 in mind, we checked several published ^{14}N NMR data of ionic and covalently bound azides and found some noticeable problems, which we do not want to discuss in detail as it is out of the focus of this work. To give one example, $Bi(N_3)_3$ is almost insoluble in CH_2Cl_2. Therefore, no ^{14}N NMR resonances can be detected.[2] However, long accumulations lead to the azido/chlorido ligand back exchange which is accompanied by the formation of HN_3 as discussed before. Interestingly, ^{14}N NMR data of $Bi(N_3)_3$ in CH_2Cl_2 have recently been published (Table 4),[3] which, however, in our opinion, must be assigned to HN_3 (vide supra). The same might be assumed for $E(N_3)_3$ (E = As, Sb, and Bi) and $Bi(N_3)_3\cdot(pyridine)_2$ all displaying almost identical ^{14}NMR data. Small deviations might be attributed to differences in the concentration, temperature, exact referencing, or the presence of traces of protic species (e.g., water). It should be noted that the azido ligand exchange reactions should also be observed in other halogenated or acidic solvents. For

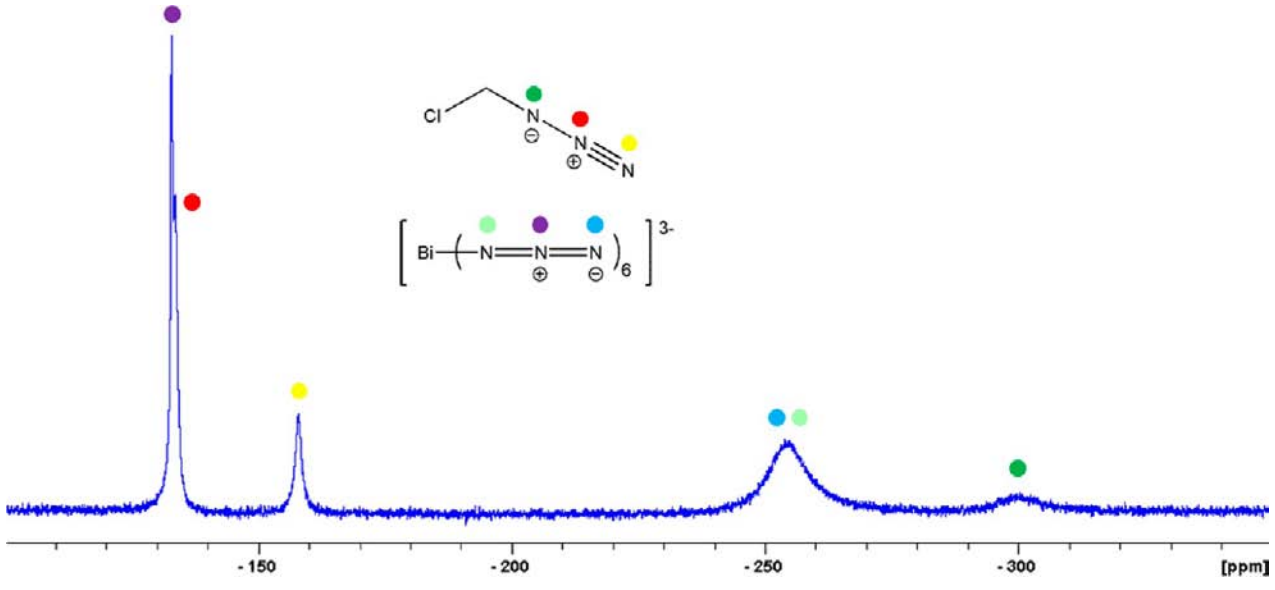

Figure 19. ^{14}N spectrum of the reaction solution of $[Ph_4P]_3[Bi(N_3)_6]$ with excess CD_2Cl_2.

dx.doi.org/10.1021/ic400493v | Inorg. Chem. 2013, 52, 6110−6126

example, our experiments with $[Ph_4P]N_3$ in $CDCl_3$ display also an azido/chloride exchange (Table 4), which, however, is much slower (Supporting Information, Figure S21) compared to CD_2Cl_2. Further temperature dependent NMR studies show that at 100 °C the exchange is accelerated, which leads to a complete conversion within 20 h. The difference between CD_2Cl_2 and $CDCl_3$ with respect to the exchange rate might be attributed to a more covalent C−Cl bond in $CDCl_3$ resulting in a larger activation barrier. Since no fast equilibration is observed at ambient temperature, once the $CD(N_3)Cl_2$ is formed at 100 °C, at ambient temperature no significant back exchange is observed even after 2 days.

Typically for covalently bound azide species, a sharp resonance is found for N_β (−110 to −150 ppm), a medium-sharp for N_γ (−145 to −250 ppm), and a broad signal for N_α (−240 to −380 ppm).[38] On the contrary, azides containing heavy elements in low oxidation states such as Sb, Bi or Se, Te,[39] mostly give rise to only two signals for N_β (−125 to −140 ppm) and $N_{\alpha/\gamma}$ (−185 to −290 ppm) with significantly larger half-width. In addition to quadrupolar broadening, fast ligand exchange on the NMR time scale especially in polar solvents such as dmso (intermolecular exchange) or the Berry pseudorotation mechanism (intramolecular exchange) can contribute to the observation of only two azide signals and the relative broadness of the $N_{\alpha/\gamma}$ resonance instead of a separate N_α and N_γ resonance.[36,40]

CONCLUSIONS

The highly explosive bismuth triazide, $Bi(N_3)_3$, was obtained in pure form by the reaction of BiF_3 with Me_3SiN_3 in acetonitrile under solvothermal conditions. $Bi(N_3)_3$ crystallizes isotypically to $Sb(N_3)_3$ (space group $P\bar{1}$) and forms similar to $Bi(N_3)_3$·acetonitrile, $Bi(N_3)_3$·acetone, and $Bi(N_3)_3$·dmso adducts a two-dimensional network which arises from three azido bridges per Bi center.

Moreover, the lone pair activity in $[Bi^{(III)}(N_3)_6]^{3-}$, which is triggered by small changes in the local environment around the ion, leads to two different isomers in the solid state, which might be regarded as bond-stretch isomers. Temperature variable single crystal X-ray studies revealed a strongly distorted low-temperature isomer with a stereochemically active lone pair localized at the $Bi^{(III)}$ center and a high-temperature isomer with an approximate O_h-symmetric BiN_6 core and a sterically inactive lone pair. The presence of a formally active lone pair in the valence shell leads to an off-centric displacement of the Bi^{3+} ion from the centroid of its formally S_6-symmetric coordination polyhedron. The observed effect seems to be the result of packing forces, that is, due to the low local symmetry at the bismuth site (space group $P\bar{1}$). Cooling down the crystal leads to an anisotropic shrinking of the unit cell axes and thus induces the lower symmetry. This lower symmetry then leads to a different character of the lone pair leading at the end to the different bond lengths.

Finally, the azido-chlorido ligand back exchange was demonstrated when chlorinated solvents such as CH_2Cl_2 were utilized leading to the formation of $CH_2(N_3)Cl$ and/or HN_3 and partially chlorinated bismuth azides. Therefore, the use of chlorine-free solvents is strongly recommended in azide chemistry especially when azido metallates are studied.

EXPERIMENTAL SECTION

Caution! *Covalent azides are potentially hazardous and can decompose explosively under various conditions! Especially $Bi(N_3)_3$ and its solvent adducts are extremely shock-sensitive and can explode violently upon the slightest provocation. Appropriate safety precautions (safety shields, face shields, leather gloves, protective clothing) should be taken when dealing with large quantities.*

Synthesis of $Bi(N_3)_3$. BiF_3 (0.066 g, 0.25 mmol) in acetonitrile (3 mL) and Me_3SiN_3 (neat, 0.285 g, 2.47 mmol) are combined at ambient temperatures in a quartz tube. The mixture is degassed several times and sealed in vacuo. Sonification in an ultrasonic bath at 90 °C for 12 h resulted in a yellow microcrystalline solid and a clear supernatant. The tube is opened in air, and the solid is quickly suspended by syringe and transferred to a Schlenk tube. The supernatant was removed by syringe, and the residue was washed with small portions of acetonitrile. Drying in vacuo gave $Bi(N_3)_3$ as an yellowish crystalline solid in almost quantitative yields. The synthesis may alternatively be carried out without ultrasonic irradiation, which allows for the usage of normal boro-silicate glass tubes. However, the product is of lower crystallinity but tends to build an agglomerate which is difficult to be ground without a violent detonation. **Mp** 191 °C (detonation). **ICP** calc. (found) g/l: Bi 0.67 (0.67). **IR** (ATR, 32 scans): 3352 (w); 3295 (w); 3271 (w); 2561 (w); 2506 (w); 2548 (w); 2506 (w); 2491 (w); 2432 (w); 2043 (s); 1330 (m); 1312 (m); 1248 (s); 1172 (m); 1161 (m); 655 (m); 647 (s); 589 (m); 583 (m). **Raman** (a: 65.1 mW, 25 °C, 2 acc., 20 s., cm^{-1}): = 2101 (4); 2067 (3); 2052 (2); 1331 (1); 1316 (1); 1269 (1); 1260 (1); 1252 (1); 650 (2); 588 (1); 339 (5); 306 (10); 247 (6); 226 (6).

Synthesis of $Bi(N_3)_3$·CH_3CN. BiF_3 (0.133 g, 0.5 mmol) is suspended in acetonitrile (2 mL), and Me_3SiN_3 (neat, 0.576 g, 5.0 mmol) is added at ambient temperatures. The colorless suspension is stirred for 4 days, resulting in a colorless solid. Removal of solvent by syringe and short drying in vacuo for 10 min gives $Bi(N_3)_3$·CH_3CN as a colorless to pale yellowish solid in almost quantitative yields. **Mp** 197 °C (detonation). **ICP** calc. (found) g/l: Bi 0.30 (0.31). **^{14}N NMR** (300 K, d_3-acetonitrile, 36.14 MHz): δ = not detected besides CD_3CN: −135 ($\Delta\nu_{1/2}$ = 83 Hz). **IR** (ATR, 32 scans): 3353 (w); 3297 (w); 3169 (w); 2993 (w); 2934 (w); 2670 (w); 2607 (w); 2564 (w); 2508 (w); 2493 (w); 2293 (w); 2254 (m); 2114 (m); 2047 (s); 1445 (w); 1406 (w); 1368 (m); 1322 (s); 1276 (m); 1259 (s); 1204 (m); 1177 (m); 1034 (m); 924 (m); 786 (w); 767 (w); 670 (w); 655 (m); 647 (s); 604 (w); 591 (m); 580 (m). **Raman** (a: 65.1 mW, 25 °C, 6 acc., 25 s., cm^{-1}): = 2998 (1); 2935 (2); 2294 (1); 2254 (3); 2205 (1); 2113 (5); 2083 (1); 2061 (1); 2043 (7); 1442 (1); 1407 (1); 1372 (1); 1367 (1); 1332 (5); 1280 (1); 1270 (1); 1262 (1); 1251 (1); 1203 (1); 1178 (1); 1034 (1); 924 (1); 767 (1); 654 (2); 605 (2); 591 (1); 579 (1); 394 (3); 385 (2); 371 (2); 339 (9); 292 (4); 271 (5); 228 (9); 207 (10); 179 (6); 155 (8).

Synthesis of $Bi(N_3)_3$·dmso. BiF_3 (0.266 g, 1.0 mmol) in dmso (3 mL) and Me_3SiN_3 (neat, 0.777 g, 0.67 mmol) are combined at ambient temperatures. The colorless suspension is stirred for 24 h resulting in a yellow solution. Removal of solvent and drying in vacuo gives $Bi(N_3)_3$·dmso as an yellowish solid in almost quantitative yields. **Mp** 199.6 °C (detonation, 160.6 °C loss of dmso). **ICP** calc. (found) g/l: Bi 0.53 (0.53) **^{14}N NMR** (300 K, d_6-dmso, 36.14 MHz): δ = −137 (N_β, $\Delta\nu_{1/2}$ = 71 Hz), −260 (N_γ, $\Delta\nu_{1/2}$ = 632 Hz). **IR** (ATR, 32 scans): 3325 (w); 3292 (w); 3017 (w); 2935 (w); 2579 (w); 2519 (w); 2074 (s); 2021 (s); 1403 (m); 1326 (m); 1315 (m); 1273 (m); 1261 (s); 1178 (w); 1020 (w); 982 (s); 937 (s); 717 (m); 672 (w); 663 (m); 655 (m); 633 (m); 611 (w); 591 (m). **Raman** (a: 65.1 mW, 25 °C, 2 acc., 20 s., cm^{-1}): = 3021 (1); 2937 (2); 2928 (2); 2103 (6); 2032 (2); 2012 (5); 2006 (3); 1420 (2); 1395 (2); 1329 (8); 1279 (2); 1267 (1); 1259 (1); 1217 (1); 1178 (1); 1017 (1); 977 (1); 943 (2); 721 (5); 682 (10); 659 (1); 652 (1); 634 (1); 612 (5); 591 (1); 420 (2); 347 (1); 321 (2); 293 (3); 231 (10).

Synthesis of $Bi(N_3)_3$·acetone. BiF_3 (0.133 g, 0.5 mmol) is suspended in acetone (5 mL) and Me_3SiN_3 (neat, 0.576 g, 5.0 mmol) is added at ambient temperatures. The colorless suspension is stirred for 4 days, resulting in a colorless solid. Removal of solvent by syringe and short drying in vacuo for 20 min gives $Bi(N_3)_3$·acetone as a colorless to pale yellowish solid in almost quantitative yields. **Mp** 227 °C (detonation). **ICP** calc. (found) g/l: Bi 0.27 (0.27) **^{14}N NMR** (300 K, d_6-acetone, 36.14 MHz): δ = not detected. **IR** (ATR, 32 scans):

dx.doi.org/10.1021/ic400493v | Inorg. Chem. 2013, 52, 6110−6126

3350 (w); 3297 (w); 2997 (w); 2920 (w); 2852 (w); 2663 (w); 2596 (w); 2574 (w); 2519 (w); 2498 (w); 2455 (w); 2114 (m); 2077 (m); 2048 (s); 1689 (s); 1653 (m); 1419 (w); 1359 (m); 1323 (s); 1273 (s); 1262 (s); 1232 (s); 1201 (m); 1180 (w); 1089 (w); 987 (w); 932 (w); 861 (w); 804 (w); 669 (m); 656 (m); 647 (w); 603 (w); 591 (w); 580 (w). **Raman** (a: 65.1 mW, 25 °C, 4 acc., 40 s., cm^{-1}): = 3011 (1); 2979 (1); 2925 (1); 2118 (3); 2085 (1); 2044 (5); 1701 (2); 1695 (1); 1421 (1); 1328 (3); 1280 (2); 1268 (1); 1255 (1); 1236 (1); 1078 (1); 803 (2); 663 (2); 654 (3); 607 (3); 531 (2); 495 (2); 412 (3); 370 (3); 331 (7); 269 (7); 232 (8); 208 (10).

Synthesis of $[Ph_4P]_3[Bi(N_3)_6]$. To a stirred orange suspension of $[Ph_4P]_3[BiI_6]$ (0.655 g, 0.5 mmol) in acetonitrile (10 mL), AgN_3 (neat, 0.541 g, 3.6 mmol) is added in one portion at ambient temperatures. The resulting yellow suspension is stirred for 1 h. The solution is filtered (F4) and strongly concentrated in vacuo to a yellow viscous oil. Crystallization may be initiated by addition of a small crystal of $[Ph_4P]_3[Bi(N_3)_6]$. Storage at ambient temperatures results in the deposition of yellow crystals. Drying in vacuo gives $[Ph_4P]_3[Bi(N_3)_6]$ as a yellow crystalline solid in almost quantitative yields. **Mp** 179 °C (285 °C dec.). **Anal. Calc.** % (found): C, 58.46 (58.15); H, 4.09 (4.36); N, 17.04 (16.59). **ICP** calc. (found) g/l: Bi 0.14 (0.15). **^{14}N NMR** (300 K, CD_3CN, 36.14 MHz): δ = −133 (N_β, partially overlapping with CH_3CN at −135), −258 (N_γ, $\Delta\nu_{1/2}$ = 140 Hz). **^{14}N NMR** (300 K, d$_6$-DMSO, 36.14 MHz): δ = −132 (N_β, $\Delta\nu_{1/2}$ = 42 Hz), −258 (N_γ, $\Delta\nu_{1/2}$ = 390 Hz). **^{14}N NMR** (300 K, CD_2Cl_2, 36.14 MHz): δ = −133 (N_β, $\Delta\nu_{1/2}$ = 28 Hz), −258 (N_γ, $\Delta\nu_{1/2}$ = 250 Hz). **IR** (ATR, 32 scans): 3300 (w); 3077 (w); 3056 (w); 2055 (m); 1994 (s); 1583 (m); 1481 (m); 1434 (s); 1312 (s); 1261 (m); 1186 (m); 1162 (m); 1104 (s); 1027 (w); 995 (s); 940 (w); 856 (w); 755 (m); 719 (s); 687 (s); 636 (m); 615 (m). **Raman** (b: 200 mW, 25 °C, 1904 scans, cm^{-1}): = 3312 (1); 3170 (1); 3144 (1); 3063 (5); 2996 (1); 2909 (2); 2063 (2); 2025 (1); 2007 (1); 1587 (4); 1485 (1); 1441 (1); 1325 (3); 1264(3); 1189 (1); 1166 (1); 1109 (1); 1100 (2); 1030 (3); 1002 (7); 944 (1); 759 (1); 726 (1); 681 (2); 637 (1); 618 (2); 396 (1); 322 (3); 293 (2); 258 (2); 198 (2); 89 (10).

Synthesis of $[EtPh_3P]_3[Bi(N_3)_6]$. To a stirred suspension of $[EtPh_3P]I$ (1.261 g, 3.01 mmol) in thf (15 mL), BiI_3 (neat, 0.592 g, 1.0 mmol) is added in one portion at ambient temperatures. The resulting red suspension is stirred for 2 h and was then shortly heated to reflux, resulting in the separation of a red oily layer. After the addition of *n*-hexane (5 mL) the supernatant is removed by decantation, and the red oil is dried in vacuo. The residue is dissolved in acetonitrile (20 mL) and to the resulting red solution, AgN_3 (neat, 1.091 g, 7.29 mmol) is added in one portion at ambient temperature. The resulting yellow suspension is stirred for 2 h and filtered. The solution is concentrated to incipient crystallization in vacuo and stored at ambient temperatures for several hours, resulting in the deposition of yellow crystals. Removal of the supernatant by decantation and drying in vacuo gives $[EtPh_3P]_3[Bi(N_3)_6]$ as a yellow, crystalline solid in good yields. **Mp** 143 °C (218 °C dec.). **Anal. Calc.** % (found): C 53.97 (53.27); H 4.53 (4.97); N 18.88 (18.89). **ICP** calc. (found) g/l: Bi 0.18 (0.19) **^{14}N NMR** (300 K; 36.1 MHz; d$_6$-dmso): δ = −134 (N_β; $\Delta\nu_{1/2}$ = 72 Hz); −260 ($N_{\alpha/\gamma}$; $\Delta\nu_{1/2}$ = 547 Hz). **^{1}H NMR** (300 K; 500.13 MHz; d$_6$-dmso): δ = 7.73−7.90 (m; 15 H; *Aryl*); 3.63 (dq; 2 H; $J(^1H\text{-}^1H)$ = 7.4 Hz; $J(^1H\text{-}^{31}P)$ = 13.3 Hz; CH_2CH_3); 1.22 (dt; 3 H; $J(^1H\text{-}^1H)$ = 7.4 Hz; $J(^1H\text{-}^{31}P)$ = 20.0 Hz; CH_2CH_3). **^{13}C NMR** (300 K; 125.8 MHz; d$_6$-dmso): δ = 134.85 (d; $^4J(^{13}C\text{-}^{31}P)$ = 2.7 Hz; *para*); 133.52 (d; $^2J(^{13}C\text{-}^{31}P)$ = 10.0 Hz; *ortho*); 130.23 (d; $^3J(^{13}C\text{-}^{31}P)$ = 12.3 Hz; *meta*); 118.23 (d; $^1J(^{13}C\text{-}^{31}P)$ = 85.4 Hz; PC); 14.42 (d; $^1J(^{13}C\text{-}^{31}P)$ = 51.4 Hz; CH_2); 6.23 (d; $^2J(^{13}C\text{-}^{31}P)$ = 5.4 Hz; CH_3). **^{31}P NMR** (300 K; 202.5 MHz; d$_6$-dmso): δ = 25.9 (s; $^1J(^{13}C\text{-}^{31}P)$ = 85.4 Hz). **IR** (ATR, 32 scans): 3307 (m); 3080 (w); 3055 (w); 3024 (w); 3009 (w); 2991 (w); 2980 (w); 2938 (m); 2904 (m); 2877 (w); 2689 (w); 2638 (w); 2588 (w); 2160(m); 2063 (m); 1998 (s); 1585 (w); 1574 (w); 1484 (w); 1434 (m); 1403 (w); 1385 (w); 1316 (m); 1265 (m); 1238 (m); 1187 (w); 1157 (w); 1110 (m); 1073 (w); 1036 (w); 1028 (w); 1012 (w); 996 (m); 985 (w); 930 (w); 850 (w); 746 (m); 736 (s); 720 (s); 690 (s); 665 (m); 640 (w); 613 (m). **Raman** (a: 65.1 mW, 25 °C, 3 acc., 10 s., cm^{-1}): = 3166 (1); 3142 (1); 3057 (3); 2977 (1); 2934 (1); 2901 (1); 2874 (1); 2093 (1); 2058 (2); 1658 (1); 1581 (3); 1525 (1); 1502 (1); 1467 (1); 1427 (1); 1409 (1); 1320 (3); 1235 (1); 1185 (1); 1157 (4); 1098 (4); 1021 (5); 992 (10); 923 (1); 866 (1); 747 (1); 716 (1); 703 (1); 682 (1); 659 (3); 608 (2); 502 (1); 479 (1); 427 (1); 374 (1); 317 (3); 248 (2); 214 (1).

Synthesis of $[Bu_4N]_3[Bi(N_3)_6]$. To a stirred suspension of $[Bu_4N]I$ (0.592 g, 1.6 mmol) in thf (15 mL), BiI_3 (neat, 0.295 g, 0.5 mmol) is added in one portion at ambient temperatures. The resulting red suspension is stirred for 2 h and silver azide AgN_3 (neat, 0.532 g, 3.5 mmol) is added in one portion at ambient temperature. The resulting yellow suspension is stirred for 2 h and filtered. The solution is concentrated to incipient crystallization in vacuo and stored at ambient temperatures for several hours, resulting in the deposition of yellow crystals. Removal of the supernatant by decantation and drying in vacuo gives $[Bu_4N]_3[Bi(N_3)_6]$ as a yellow, crystalline solid in good yields. **Mp** 197 °C (dec.). **Anal. Calc.** % (found): C 48.51 (48.01); H 9.16 (8.86); N 24.75 (23.44). **ICP** calc. (found) g/l: Bi 0.17 (0.15) **^{14}N NMR** (300 K; 36.1 MHz; CD_3CN): δ = −133 (N_β; partially overlapping with CH_3CN at −135); −262 ($N_{\alpha/\gamma}$; $\Delta\nu_{1/2}$ = 230 Hz); −315 ($[Bu_4N]^+$; $\Delta\nu_{1/2}$ = 2 Hz). **^{1}H NMR** (300 K; 500.13 MHz; CD_3CN): δ = 0.93 (m; 12 H; $[(CH_3CH_2CH_2CH_2)_4N]^+$); 1.34 (m; 8 H; $[(CH_3CH_2CH_2CH_2)_4N]^+$); 1.59 (m; 8 H; $[(CH_3CH_2CH_2CH_2)_4N]^+$); 3.14 (m; 8 H; $[(CH_3CH_2CH_2CH_2)_4N]^+$). **^{13}C NMR** (300 K; 125.8 MHz; CD_3CN): δ = 14.0 ($[(CH_3CH_2CH_2CH_2)_4N]^+$); 20.0 ($[(CH_3CH_2CH_2CH_2)_4N]^+$); 24.4 ($[(CH_3CH_2CH_2CH_2)_4N]^+$); 59.2 ($[(CH_3CH_2CH_2CH_2)_4N]^+$). **IR** (ATR, 32 scans): 3382 (w); 3301 (w); 3215 (w); 2959 (m); 2935 (m); 2873 (m); 2738 (w); 2640 (w); 2592 (w), 2064 (m); 1996 (s); 1486 (m); 1457 (m); 1435 (m); 1381 (m); 1315 (m); 1266 (m); 1151 (m); 1110 (m); 1053 (m); 1026 (m); 997 (w); 952 (w); 882 (m); 799 (w); 747 (m); 737 (m); 722 (m); 690 (m); 667 (w); 635 (w); 614 (w); 528 (m). **Raman** (a: 65.1 mW, 25 °C, 4 acc., 30 s., cm^{-1}): = 2960 (1); 2928 (2); 2875 (2); 2730 (1); 2056 (2); 2003 (1); 1474 (1); 1462 (1); 1442 (2); 1315 (4); 1264 (1); 1146 (1); 1123 (1); 1048 (1); 1025 (1); 1002 (1); 902 (2); 874 (1); 793 (1); 627 (2); 319 (10); 255 (2).

Synthesis of $[Me_4N]_3[Bi(N_3)_6]$. $[Me_4N]I$ (0.306 g, 1.52 mmol) and BiI_3 (neat, 0.295 g, 0.5 mmol) are combined and dissolved in acetonitrile/dmso (2:1, 15 mL) at ambient temperatures. The resulting orange-red solution is stirred for 30 min and AgN_3 (neat, 0.521 g, 3.5 mmol) is added in one portion at ambient temperature. The resulting yellowish suspension is stirred for 1 h and filtered. The yellow solution is concentrated to an approximate volume of 1.5 mL in vacuo and stored at ambient temperatures for several hours, resulting in the deposition of colorless crystals. The crystals could be identified as $[Me_4N]N_3$ by an X-ray unit cell determination. However, the NMR spectra differ significantly from $[Me_4N]N_3$ and $Bi(N_3)_3$·dmso which clearly demonstrates the formation of $[Me_4N]_3[Bi(N_3)_6]$ in solution. **^{14}N NMR** (300 K; 36.1 MHz; d$_6$-dmso): δ = −134 (N_β; $\Delta\nu_{1/2}$ = 47 Hz); −265 ($N_{\alpha/\gamma}$; $\Delta\nu_{1/2}$ = 320 Hz); −338 ($[Me_4N]^+$; $\Delta\nu_{1/2}$ = 2 Hz). **^{1}H NMR** (300 K; 500.13 MHz; d$_6$-dmso): δ = 3.1 (s; 16 H; $[(CH_3)_4N^+$, $^1J(^{13}C\text{−}^1H)$ = 144 Hz]. **^{13}C NMR** (300 K; 125.8 MHz; d$_6$-dmso): δ = 40.4 ($[(CH_3)_4N]^+$, $^1J(^{13}C\text{−}^{14}N)$ = 80 Hz).

Computational Details. Gas phase computations (with the Gaussian program suite)[43] have been carried out for the $[Bi(N_3)_6]^{3-}$ anion and $Bi(N_3)_3$ utilizing three different DFT methods (B3LYP, pbe1pbe, and M06-2X) and an aug-cc-pvTZ-basis set for the N atoms and for Bi a fully relativistic pseudopotential (Bi: ECP60MDF) and a cc-pVTZ basis set (Bi: (12s11p9d1f)/ [5s4p3d1f]).[44] While at the B3LYP and pbe1pbe level, the S_6-symmetric isomer was found to be a minimum (no imaginary frequency) at the potential energy surface (PES), for the M06-2X methods two very small imaginary frequencies were obtained (−4 and −3 cm^{-1}). Since all these methods were neither developed nor validated for a triply negatively charged anion in the gas phase, the quality of the results cannot be judged. The computational problem is even more complex, since the PES of the $[Bi(N_3)_6]^{3-}$ anion is extremely flat, so that polarization effects, dispersion, electron correlation, and basis set effects including relativistic effects must be considered. For instance, calculations of the electronic structure of some of AX_6E systems shows that

dx.doi.org/10.1021/ic400493v | *Inorg. Chem.* 2013, 52, 6110−6126

correlation and relativistic effects diminish the pseudo-Jahn−Teller distortions stabilizing nondistorted octahedral configurations (for this reason RuF_6, $[AtF_6]^-$, and $[PoF_6]^{2-}$ emerge as regular octahedra).[28] Therefore solid state effects such as cation···anion interactions may have a huge influence. Nevertheless, experimental structural data obtained from X-ray studies are available and were used for NBO[14,15] analyses to study polarization and hybridization effects. Although the presence of 7.2 non-Lewis electrons is found for $[Bi(N_3)_6]^{3-}$ (the Rydberg non-Lewis contribution is neglible), these data can still be used to qualitatively discuss the hybridization of the lone pair localized at the Bi atom. *Note:* The large non-Lewis contribution is mainly caused by the two 4-electron-3-center bonds in each of the six azido ligands and does not really affect the situation on the Bi center. For comparison, for the N_3^- ion a non-Lewis contribution of 1.35 electrons is found. In addition, ELF computations have been performed to localize the lone pair located at the Bi center.[45−47]

■ ASSOCIATED CONTENT

Supporting Information

The Supporting Information include the following: (1) Experimental details, (2) crystallographic information, and (3) further experimental and computational data of all considered species along with all spectra. This material is available free of charge via the Internet at http://pubs.acs.org.

■ AUTHOR INFORMATION

Corresponding Author

*E-mail: axel.schulz@uni-rostock.de (A.S.), alexander.villinger@uni-rostock.de (A.V.).

Notes

The authors declare no competing financial interest.

■ ACKNOWLEDGMENTS

Fabian Reiß (University Rostock) is acknowledged for the measurement of Raman spectra, Prof. Dr. Detlef Heller and Anja König (Leibniz Institute for Catalysis Rostock) for the kinetic modeling of the azido-chlorido back exchange reaction, and Dr. Dirk Michalik (University Rostock) for NMR measurements. We thank the DFG (grant SCHU 1170 8-1), the University of Rostock, and the Leibniz Institute for Catalysis for financial support.

■ REFERENCES

(1) Klapötke, T. M.; Schulz, A. *Main Group Met. Chem.* **1997**, *20*, 325.
(2) Villinger, A.; Schulz, A. *Angew. Chem., Int. Ed.* **2010**, *49*, 8017.
(3) Schulz, S.; Lyhs, B.; Jansen, G.; Bläser, D.; Wölper, C. *Chem. Commun.* **2011**, *47*, 3401.
(4) Haiges, R.; Rahm, M.; Dixon, D. A.; Garner, E. B., III; Christe, K. O. *Inorg. Chem.* **2012**, *51*, 1127.
(5) Schulz, A.; Villinger, A. *Chem.—Eur. J.* **2012**, *18*, 2902.
(6) Challenger, F.; Richards, O. V. *J. Chem. Soc.* **1934**, 405.
(7) Müller, J. *Z. Anorg. Allg. Chem.* **1971**, *381*, 103.
(8) Dehnicke, K. *Z. Anorg. Allg. Chem.* **1974**, *409*, 311.
(9) Raj, P.; Singhal, E.; Rastogi, R. *Polyhedron* **1986**, *5*, 677.
(10) Schulz, A.; Villinger, A. *Organometallics* **2011**, *30*, 284.
(11) Berry, R. S. *J. Chem. Phys.* **1960**, *32*, 933.
(12) Haiges, R.; Vij, A.; Boatz, J. A.; Schneider, S.; Schroer, T.; Gerken, M.; Christe, K. O. *Chem.—Eur. J.* **2004**, *10*, 508.
(13) This possibility was ruled out by CHR.
(14) Pyykkö, P.; Atsumi, M. *Chem.—Eur. J.* **2009**, *15*, 12770.
(15) (a) Glendening, E. D.; Reed, A. E.; Carpenter, J. E.; Weinhold, F. *NBO*, Version 3.1; (b) Carpenter, J. E.; Weinhold, F. *J. Mol. Struct. (Theochem)* **1988**, *169*, 41. (c) Weinhold, F.; Carpenter, J. E. *The Structure of Small Molecules and Ions*; Plenum Press: New York, 1988; p 227; (d) Weinhold, F.; Landis, C. *Valency and Bonding. A Natural Bond Orbital Donor-Acceptor Perspective*; Cambridge University Press: Cambridge, U.K., 2005; and references therein.
(16) Glendening, E. D.; Badenhoop, J. K.; Reed, A. E.; Carpenter, J. E.; Bohmann, J. A.; Morales, C. M.; Weinhold, F. *NBO 5.9.* ; Theoretical Chemistry Institute, University of Wisconsin: Madison, WI, 2009; http://www.chem.wisc.edu/~nbo5
(17) Mantina, M.; Chamberlin, A. C.; Valero, R.; Cramer, C. J.; Truhlar, D. G. *J. Phys. Chem. A* **2009**, *113*, 5806.
(18) Weitze, A.; Blaschette, A.; Henschel, D.; Jones, P. G. *Z. Anorg. Allg. Chem.* **1995**, *621*, 229.
(19) Koch, G.; Ruck, M. *Z. Anorg. Allg. Chem.* **2010**, *636*, 1987.
(20) (a) Data were taken from this work. In the 2010 paper 2.719(5) and 2.326(7) Å were determined, which are identical within standard deviation; (b) A second azide group (N4/N5/N6) also exhibits a disorder, however, without variation of Bi-N distances.
(21) In the Supporting Information we mentioned, that the reaction can be carried out either in CH_2Cl_2, thf, or acetonitrile. Unfortunately, we have not mentioned that the crystal was obtained from an acetonitrile reaction.
(22) Van Gunsteren, W. F. *Angew. Chem., Int. Ed.* **2013**, *52*, 118.
(23) For comparison: A stereochemically active lone pair at bismuth is also observed within high pressure modifications of BiB_3O_6. See Roeßner, F.; Jakob, S.; Johrendt, D.; Kinski, I.; Glaum, R.; Huppertz, H. *Angew. Chem., Int. Ed.* **2006**, *46*, 9097.
(24) Orgel, L. E. *J. Chem. Soc.* **1959**, *4*, 3815.
(25) (a) Pilmé, J.; Robinson, E. A.; Gillespie, R. J. *Inorg. Chem.* **2006**, *45*, 6198. (b) Gillespie, R. J.; Robinson, E. A. *Chem. Soc. Rev.* **2005**, *34*, 396.
(26) Brown, I. D. *J. Phys. Chem. A* **2011**, *115*, 12638.
(27) Gourlaouen, C.; Parisel, O.; Gérard, H. *Dalton Trans.* **2011**, *40*, 11282.
(28) Shimoni-Livny, L.; Glusker, J. P.; Bock, C. W. *Inorg. Chem.* **1998**, *37*, 1853.
(29) (a) Gillespie, R. J.; Nyholm, R. S. *Q. Rev. Chem. Soc.* **1957**, *61*, 339. (b) Gillespie, R. J.; Robinson, E. A. *Angew Chem. Int. Ed.* **1996**, *35*, 495.
(30) Bersuker, I. B. *The Jahn-Teller Effect and Vibronic Interactions in Modern Chemistry*; Plenum: New York, 1984.
(31) Bersuker, I. B. *Chem. Rev.* **2001**, *101*, 1067.
(32) Comba, P.; Hauser, A.; Kerscher, M.; Pritzkow, H. *Angew. Chem., Int. Ed.* **2003**, *42*, 4536.
(33) (a) Parkin, G. *Chem. Rev.* **1993**, *93*, 887. (b) Rohmer, M. M.; Benard, M. *Chem. Soc. Rev.* **2001**, *30*, 340.
(34) CHR gave in their *Inorganic Chemistry* paper as reference: Haiges, R.; Vij, A.; Christe, K. O. unpublished observations.
(35) (a) Beck, W.; Fehlhammer, W. P.; Feldl, K.; Klapötke, T. M.; Kramer, G.; Mayer, P.; Piotrowski, H.; Pöllmann, P.; Ponikwar, W.; Schütt, T.; Schuierer, E.; Vogt, M. *Z. Anorg. Allg. Chem.* **2001**, *627*, 1751. (b) Müller, U.; Dehnicke, K. *Angew. Chem., Int. Ed.* **1966**, *5*, 841. (c) Neumüller, B.; Schmock, F.; Schlecht, S.; Dehnicke, K. *Z. Anorg. Allg. Chem.* **2000**, *626*, 1792. (d) Kolitsch, W.; Müller, U. *Z. Anorg. Allg. Chem.* **1974**, *410*, 21.
(36) Banert, K.; Joo, Y.-H.; Rüffer, T.; Walfort, B.; Lang, H. *Tetrahedron Lett.* **2010**, *51*, 2880.
(37) Evers, J.; Göbel, M.; Krumm, B.; Martin, F.; Medvedyev, S.; Oehlinger, G.; Steemann, F. X.; Troyan, I.; Klapötke, T. M.; Eremets, M. I. *J. Am. Chem. Soc.* **2011**, *133*, 12100.
(38) Tornieporth-Oetting, I.-C.; Klapötke, T. M. *Angew. Chem., Int. Ed.* **1995**, *34*, 512.
(39) Haiges, R.; Boatz, J. A.; Vij, A.; Gerken, M.; Schneider, S.; Schroer, T.; Christe, K. O. *Angew. Chem., Int. Ed.* **2003**, *42*, 5843.
(40) Berry, R. S. *J. Chem. Phys.* **1960**, *32*, 933.
(41) Klapötke, T. M.; Geissler, P. *J. Chem. Soc., Dalton Trans.* **1995**, 3365.
(42) Geissler, P.; Klapötke, T. M.; Kroth, H.-J. *Spectrochim. Acta* **1995**, *51A*, 1075.
(43) Frisch, M. J. et al. *Gaussian 09*, Revision A.02; Gaussian, Inc.: Wallingford, CT, 2009.
(44) Peterson, K. A. *J. Chem. Phys.* **2003**, *119*, 11099.

(45) Silvi, B.; Savin, A. *Nature* **1994**, *371*, 683.
(46) Grützmacher, H.; Fässler, T. F. *Chem.—Eur. J.* **2000**, *6*, 2317.
(47) *Multiwfn*, Version 2.2; Lu, T.; Chen, F. *J. Comput. Chem.* **2012**, *33*, 580.